

Thank you for your comments. We have replied your comments as follows. We show your comments and our replies in black and blue texts, respectively.

In this study, the authors estimated the long-term trends of pH in Japanese coastal waters from 1978 to 2009. In 70 to 75 % of the monitored sites, they found acidification trends while they obtained basification trends in 25 to 30 % of the sites. The authors tried to interpret the spatio-temporal patterns in pH based on the in situ pH, temperature and total nitrogen data. The paper's idea is very important taking into consideration the increasing need of a continuous OA monitoring, particularly in coastal areas where OA effects on marine ecosystems could be exacerbated due to local pressures. However, I do have some major concerns about the pH data and the methodology used to get it:

1) Are the authors calibrating the glass electrode with TRIS solutions for seawater measurements? I'm not against NBS standard buffers for experimental essays or to check the in situ variations of pH in coastal stations to assess the pollution there or whatsoever, but pH potentiometric measurements with NBS calibrations are strictly not recommended for seawater monitoring, particularly for long term surveys (climatic survey) where the pH uncertainty should be around 0.003 pH unit. Moreover, this technique's results are not comparable with the ones adopted for seawater elsewhere and mentioned in the entire text (i.e. Bates et al., 2014, etc.). Please check the following useful links for the recommended strategies to better study the OA in open and coastal areas for long or short periods: - http://goa-on.org/documents/general/GOA-ON_Implementation_Strategy.pdf - http://goa-on.org/resources/sdg_14.3.1_indicator.php

Thank you for your information of the links to the monitoring strategies recently recommended by GOA-ON for studying the ocean acidification. We understand that the NBS standard buffers are not appropriate for long-term monitoring focusing on climatic survey as we described in the introduction (Chapter 1). However, widespread use of seawater-scale pH buffers started in 1994 (Dickson and Goyet, 1994). This means that we MUST use NBS-scaled pH data if we want to analyze interannual variation of pH with time scale longer than 25 years.

The WPCL program fully realizes uncertainty of their seawater pH data, and this is because they set their permissible range of pH data as 0.1 pH. This precision is, of course, far insufficient to assess a temporal trend of a single station. We, therefore, focus on statistical characteristics of all derived trends instead of assessing each single trend. We demonstrate in section 4.1 that even if each trend at each site involves non-negligible measurement error, evaluation of whole statistical characteristics of the population (group) is feasible. To clarify the punch-line of our study, we have added new descriptions, especially in Section 4.2.

In summary, we propose here one practicable way to extract some meaningful information from past NBS-scale pH datasets. We believe this approach more useful than just revoking all past NBS-scale pH data.

2) The authors did not explain why they calculated trends for minimum and maximum pH values? Why didn't you calculate the trends based on the annual average pH instead of doing it for the minimum and maximum values separately?

As described in Section 2.1, the WPCL pH dataset contains only the annual minimum and maximum pH data without any information of the detailed measurement time. We assume that basically the annual minimum and maximum represents summer pH of 10m water and winter pH of surface water, respectively. As these two valuables represent pH trends at different water depths, we did not calculate average of these values. Moreover, the situation would be different at each site in summer and winter; therefore we calculated trends for minimum and maximum pH values separately. For example, in summer, biological activity would be more active but in winter, winter mixing would be more active. Such situation should be totally different from each other. Our analysis results of thermal effects on the trends are consistent with our assumption that annual minimum and maximum pH were measured in summer and winter, respectively.

3) The authors are relying on this methodology: ISO10523 (<https://www.iso.org/standard/51994.html>) mentioned in P7, L135. This method is adopted mainly for freshwater measurements. Could you please provide more information about the JIS Z8802 standard protocol (2011). It is apparently accredited in JIS list (<file:///C:/Users/user/Downloads/jis-japanese-industrial-standards.pdf>; p397) but I couldn't find its details.

ISO10523 is the methodology mainly adopted for freshwater measurements, but as we mentioned in the reply 1), this method had been adopted also for seawater measurement until 1994. JIS Z8802 is Japanese standard protocol that is formally compatible with ISO 10523. WPCL adopted this methodology for seawater pH measurement as it has launched in 1970, and they had not changed the methodology to maintain continuity in the measurements. We are now proposing to Japan Ministry of Environment to add pH measurements with present standard methods (ca. Dickson, Sabine and Christian 2007) in some coastal stations, but so far, only available dataset is the presented ISO10523-based dataset.

4) Any inter-calibration essays have been conducted to compare the pH results between the licensed operators/ labs?

We have found no information about inter-calibration essays between the licensed operators/labs in the WPCL program. We suppose that inter-calibration essays have not been conducted. To check the data quality by ourselves, we compared the pH trends measured by different licensed operators (see Section 2.2 and Fig. 6) and processed the data selection by the multi-step quality checking procedure.

5) How did you correlate the pH trends to biological processes? Did you check the correlation between pH and biological parameters measured in parallel at the monitored sites?

Since the pH data under the WPCL program were measured for monitoring the pollution control, the proper biological parameters were basically not included in the targets of the monitoring. Only the Total Nitrogen (TN) data are available from the data archive for a period from 1981 to 1995. We thus use them for the relevant discussion in section 4.2.2.

As mentioned by other reviewer, pH minimum substantially represents summer pH of subsurface (10m) water, so this trend shows negative correlation with that of TN. This relationship had partly offset anthropogenic-CO₂ induced pH decrease, because TN loadings to Japan coastal waters had significantly decreased in recent years.

6) How the dominance of heterotrophs or autotrophs might affect the pH in coastal waters? How did you related these to your data? Based on what have you suggested that these waters are oligotrophic? Many statements through the text are so weak and need to be better justified.

To consider possible causes leading to contrast in acidification and basification trends among the sites, we assume that the eutrophication enhances acidification (basification) in the heterotrophic (autotrophic) sites (Duarte et al. 2013). We show that the assumption is partly confirmed by checking the negative correlation between pH and TN trends (Table 3). Figure 14 also indicates that some of the sites involve combination of negative (positive) pH and positive (negative) TN trends, suggesting the heterotrophic condition at the sites. The autotrophic condition is suggested by the sites shown in the second and fourths quadrants (Fig.14). We have modified the relevant descriptions to more elucidate this point.

Figures: The style of many figures is very confusing, also their captions! For Fig. 6 for example,

the same-color lines indicate the pH values taken for the same place and the same operator, but one for the annual maximum and another one for the annual minimum pH? This was understood from the Fig. 6 caption, but not from the text. Please rephrase.

We have added some explanations about the annual and minimum pH_{insitu} data in caption of Fig. 6. The captions of other figures were also reconsidered. Thank you for your indication.

Tables: Table 2: How significant were these correlations? Why you didn't present this table the way you did in Table 3?

We have added information about the significance in Table 2.

Replies for the specific comments in your attached document.

L81-L85: Too much info. about only one region "Chesapeake Bay, US".

This part has been removed in the present version.

L310-L312: This sentence is very confusing!

We have revised this part in the present manuscript as follows.

“In the waters where primary productivity is predominantly to organic decomposition (i.e., autotrophic water), N increase will enhance primary production and hence decrease DIC, causing basification. In the adjoining waters of this autotrophic watermass, however, N increase will arise increase of POC transport from the autotrophic watermass, and this leads increase of POC-decomposed DIC (i.e., heterotrophic water) and cause acidification (e.g., Sunda and Cai 2012; Duarte et al. 2013).”

L314-L317: These statements need to be related to your data.

This part is surely related to the analyses focusing on the distributions of the whole pH trends. We modified it to more emphasize our viewpoint.

L332-L335: In the rest of this section, you have assessed the thermal effect on pH trends by

normalizing the pH_{insitu} to pH₂₅. How did you test the second assumption related to the coastal carbon cycle?

We have modified the relevant description to clarify the logical structure. We first examine the thermal effect (D (T)) targeting the whole populations of pH_{insitu} trends, and then check ocean acidification effect (DIC (AirCO₂)) for the populations of pH₂₅ trends after normalization. Variability inside of the trend populations comes from the regional differences in the trends, which would be affected by other factors.

L356: The captions in your figures need to be clearer, so each color should be better assigned to a specific parameter. Also, please replace "deg" for Temperature by "°C".

The captions in the all figures were reconsidered, being improved. We have replaced “deg. C” for "°C" in the present manuscript.

L380-L381: Mixing the values/trends of both minimum pH_{insitu} and maximum pH_{insitu} is very confusing through the entire text. This needs to be improved.

We have unified to use the ‘trends’ in the present manuscript.

L407-409 how the dominance of heterotrophs or autotrophs might affect the pH in coastal waters? How did you relate these to your data? Based on what have you suggested that these waters are oligotrophic? These statements are so weak and need to be better justified.

We simply speculate possible existence of the heterotrophic and autotrophic sites according to Figure 14. Also see our reply comment to item 6).

L414 : This is weird. Do you mean oligotrophic and eutrophic waters?

We mean heterotrophic and autotrophic conditions for categorization of each site. A heterotrophic site shows a negative (positive) pH trend by responding to an eutrophication (oligotrophication) trend, and vice versa for an autotrophic site.

L451: I think you mean the trophic state index of the waters.

Yes, our categorization of heterotrophic/autotrophic sites is based on basically same

terminology.

Please also note the supplement to this comment:

[://www https.biogeosciences-discuss.net/bg-2019-150/bg-2019-150-RC1-supplement.pdf](https://www.https.biogeosciences-discuss.net/bg-2019-150/bg-2019-150-RC1-supplement.pdf)

Thank you for careful checking of our manuscript. It was very helpful for improving the description.

Interactive comment on Biogeosciences Discuss., <https://doi.org/10.5194/bg-2019-150>, 2019.

1 Long-term trends in pH in Japanese coastal sea waters

2
3 Miho Ishizu¹, Yasumasa Miyazawa¹, Tomohiko Tsunoda², Tsuneo Ono³

4
5 ¹E-mail: mishizu@jamstec.go.jp

6 ¹E-mail: miyazawa@jamstec.go.jp

7 Japan Agency for Marine-Earth Science and Technology, Environmental Variability Prediction and
8 Application Research Group, Yokohama Institute for Earth Sciences, 3173-25 Showa-machi,
9 Kanagawa-ku, Yokohama 236-0001, Japan

10 Tel: +81-45-778-5875

11 Fax: +81-45-778-5497

12

13 ²E-mail: t-tsunoda@spf.or.jp

14 The Ocean Policy Research Institute of the Sasakawa Peace Foundation, 1-15-16, Toranomom Minato-
15 ku, Tokyo 105-8524, Japan

16

17 ³E-mail: tono@affrc.go.jp

18 Japan Fisheries Research Education Agency, 15F Queen's Tower B, 2-3-3 Minato Mirai, Nishi-ku,
19 Yokohama, Kanagawa 220-6115, Japan

20

21 **Abstract**

22 In recent decades, acidification of the open ocean has shown consistent increases. However,
23 analysis of long-term data in coastal sea waters shows that the pH is highly variable because of coastal

24 processes and anthropogenic carbon inputs. It is therefore important to understand how anthropogenic
25 carbon inputs and other natural or anthropogenic factors influence the temporal trends in pH in coastal
26 sea waters. Using water quality data collected at 289 monitoring sites as part of the Water Pollution
27 Control Program, we determined the long-term trends of $\text{pH}_{\text{insitu}}$ in Japanese coastal sea waters at
28 ambient temperature from 1978 to 2009. We found that $\text{pH}_{\text{insitu}}$ decreased (i.e., acidification) at
29 between 70% and 75% of the sites and increased (i.e., basification) at between 25% and 30% of the
30 sites. The rate of decrease varied seasonally and was, on average, -0.0014 yr^{-1} in summer and -0.0024
31 yr^{-1} in winter, but with relatively large deviations from these average values. The seasonal variation in
32 the average $\text{pH}_{\text{insitu}}$ trends reflects variability in warming trends. The trend distributions of pH
33 normalized at 25 deg. C also showed negative shifts, suggesting indication of ocean acidification that
34 has occurred in Japanese coastal sea waters.

35

36 Keywords: pH, CO₂, Global warming, Ocean acidification, Coastal
37 acidification/basification, Data analysis

38

39 1. Introduction

40 The effect of ocean acidification on several marine organisms, including calcifiers, is widely
41 acknowledged and is the topic of various marine research projects worldwide. Chemical variables
42 related to carbonate cycles are monitored in several ongoing ocean projects to determine whether the

43 rate of ocean acidification can be identified from changes in pH and other variables in the open ocean
44 (Gonzalez-Davila et al. 2007; Dore et al. 2009; Bates 2007; Bates et al. 2014; Midorikawa et al. 2010;
45 Olafsson et al. 2009; Wakita et al. 2017). Analysis of pH data measured in situ at the European Station
46 in the Canary Islands (ESTOC) in the North Atlantic from 1995 to 2003 and normalized to 25 deg. C
47 showed that pH_{25} decreased at a rate of $0.0017 \pm 0.0005 \text{ yr}^{-1}$ (Gonzalez-Davila et al. 2007). Similarly,
48 analysis of the Hawaii Ocean Time-series (HOT) (Dore et al. 2009) and the Bermuda Atlantic Time
49 Series (BATS) (Bates 2007) showed that pH at ambient (in-situ) sea surface temperature ($\text{pH}_{\text{insitu}}$)
50 decreased by 0.0019 ± 0.0002 and $0.0017 \pm 0.0001 \text{ yr}^{-1}$ from 1988 to 2007 and from 1983 to 2005,
51 respectively. Analysis of data collected along the hydrographic observation line at 137°E in the western
52 North Pacific by the Japanese Meteorological Agency (JMA) showed that pH_{25} decreased by
53 $0.0013 \pm 0.0005 \text{ yr}^{-1}$ in summer and $0.0018 \pm 0.0002 \text{ yr}^{-1}$ in winter from 1983 to 2007 (Midorikawa et
54 al. 2010). The winter $\text{pH}_{\text{insitu}}$ in surface water in the Nordic Seas decreased at a rate of 0.0024 ± 0.0002
55 yr^{-1} from 1985 to 2008 (Olafsson et al. 2009). This rate was somewhat more rapid than the average
56 annual rates calculated for the other subtropical time-series stations in the Atlantic Ocean, BATS, and
57 ESTOC, and was attributed to the air–sea CO_2 flux and buffering capacity (higher Revelle factor)
58 (Olafsson et al. 2009), which were higher and lower than those in subtropical regions, respectively.
59 Wakita et al. (2017) estimated that the annual and winter $\text{pH}_{\text{insitu}}$ at station K2 in the subarctic western
60 North Pacific decreased at rates of 0.0025 and 0.0008 yr^{-1} , respectively, from 1999 to 2015. The lower
61 rate in winter was explained by increases in dissolved inorganic carbon (DIC) and total alkalinity (Alk)

62 that resulted from climate-related variations in ocean currents.

63 These long-term time-series from various sites in the open ocean indicate consistent changes in
64 surface ocean carbon chemistry, which mainly reflect the uptake of anthropogenic CO₂, with
65 consequences for ocean acidity. Coastal [sea](#) waters, however, differ from the open ocean as they are
66 subjected to multiple influences, such as hydrological processes, land use in watersheds, nutrient inputs
67 (Duarte et al. 2013), changes in the structure of ecosystems caused by eutrophication (Borges and
68 Gypens 2010; Cai et al. 2011), marine pollution (Zeng et al. 2015), and variations in salinity (Sunda
69 and Cai 2012).

70 Duarte et al. (2013) hypothesized that anthropogenic pressures would cause the pH_{insitu} of coastal
71 [sea](#) waters to decrease (acidification) or increase (basification), depending on the balance between the
72 atmospheric CO₂ inputs and watershed exports of alkaline compounds, organic matter, and nutrients.
73 [For example, in Chesapeake Bay, trends in pH_{insitu} have shown temporal variations over the last 60](#)
74 [years, presumably because of the combined influence of increases and decreases in pH_{insitu} in the](#)
75 [mesohaline and polyhaline regions of the mainstem of the bay, respectively \(Waldbusser et al. 2011;](#)
76 [Duarte et al. 2013\).](#)

77 These processes that occur only in coastal regions might cause increases or decreases in the rate of
78 acidification, meaning that the outcomes for coastal ecosystems in different regions will vary. At
79 present we have limited information about long-term changes in pH in coastal [sea](#) waters, mainly
80 because of the difficulty involved in collecting continuous long-term data from coastal [sea](#) waters

81 around an entire country at a spatial resolution that is sufficient to cover the high regional variability
82 in coastal pH.

83 The Water Pollution Control Law (WPCL) was established in 1970 to deal with the serious
84 pollution of the Japanese aquatic environment in the 1950s and 1960s. Several environmental variables,
85 including $\text{pH}_{\text{insitu}}$, have been continuously measured in coastal waters since 1978, using consistent
86 methods enacted in the monitoring program [under the government leadership](#), to help protect coastal
87 water and groundwater from pollution and retain the integrity of water environments. The errors in pH
88 measurements collected in this program were assessed as outlined in the JIS Z8802 (JIS; Japanese
89 Industrial Standard) standard protocol (2011) that corresponds to the ISO 10523 (ISO; International
90 Organization for Standardization) standard protocol. Compared with the specialized oceanographic
91 protocols described in the United States Department of Energy (DOE) Handbook (1994), it is not
92 difficult to achieve the JIS protocol. The JIS and DOE standard protocols allow measurement errors of
93 less than ± 0.07 and ± 0.003 , respectively, for the glass electrode method, and the DOE protocol
94 demands a precision of ± 0.001 for the spectrophotometric method. Measurements are generally made
95 with the higher-quality spectrophotometric method during major oceanographic studies (e.g.
96 Midorikawa et al. 2010). The coastal monitoring program in Japan comprises more than 2000
97 monitoring sites that cover most parts of the coastline (Fig. 1), so the dataset provides the opportunity
98 to estimate the overall trend in pH in Japanese coastal areas and the regional variability in the trends
99 from data with a known precision.

100 In the present study, we examined the $\text{pH}_{\text{insitu}}$ trends in surface coastal sea waters from data
101 measured as part of WPCL monitoring programs. We then examined the trends at specific locations.
102 The remainder of this manuscript is organized as follows: the data and methods are described in Section
103 2, and trends in $\text{pH}_{\text{insitu}}$ are presented in Section 3, the results are discussed in Section 4 and the
104 concluding remarks are provided in Section 5.

105

106 2. Materials and Methods

107 2.1 Water Pollution Control Law (WPCL) monitoring data

108 Data for several environmental variables, including $\text{pH}_{\text{insitu}}$, and the associated metadata, are
109 available on the website of the National Institute for Environmental Studies (www.nies.go.jp/igreen;
110 http://www.nies.go.jp/igreen/md_down.html). We downloaded data for $\text{pH}_{\text{insitu}}$ from 1978 to 2009 for
111 the trend analysis. We also downloaded temperature (T) and total nitrogen (TN) data that were
112 measured at the same sites as the $\text{pH}_{\text{insitu}}$ data for the same time period (data for T and TN from 1981
113 to 1995 were available), to check the quality of the $\text{pH}_{\text{insitu}}$ data (Section 2.2), and to discuss coastal
114 processes that influenced the $\text{pH}_{\text{insitu}}$ (Section 4.2).

115 The data were collected by the Regional Development Bureau of the Ministry of Land,
116 Infrastructure, Transport and Tourism, and the Ministry of the Environment under the WPCL
117 monitoring program. Monitoring protocols (sampling frequencies, locations, and methods) are outlined
118 in the program guidelines (NIES 2018; MOE 2018) written in Japanese, and here we summarize these

119 protocols.

120 Monitoring operations are occupied at 1481 sites along the Japan coast shown in Figure 1a. Most
121 stations locate coastal area while <10 % of the station locates estuary. In each monitoring sites, basic
122 surveys were held 4 to 40 times a year dependent to the site. Information on the sampling frequency at
123 the monitoring sites is presented in Table 1. At each basic survey, water samples were collected at
124 several depths (0.5 and 2.0 m below the surface for all sites, and 10 m where the bottom depth was
125 more than this) four times a day to cover diurnal variation. At sites where large variation is found in
126 the daily pH data, additional one day water sampling at 2-hourly intervals (ca. 13 times a day) was
127 made at least twice a year to check the adequacy of basic water sampling protocol.

128 Measurements of pH for each water sample were made following the Japanese Industrial
129 Standard protocol JIS Z 8802 (2011), which is equivalent to ISO10523
130 (<https://www.iso.org/standard/51994.html>). Namely, pH was measured by glass electrode calibrated
131 by NBS standard buffers. Basically, pH measurement was carried out just after the water sampling at
132 in-situ water temperature. Permitted repeatability in each measurement was ± 0.07 . NIES gathered all
133 pH data measured at each site and calculated annual minimum and maximum pH, providing them
134 through their website.

135 The published WPCL pH dataset only contains these annual minimum and maximum pH data in
136 each year, reported on the NBS pH scale ($\text{pH}_{\text{in situ}}$) and rounded to one decimal place. Water temperature
137 data are also available for each sampling event (http://www.nies.go.jp/igreen/md_down.html).

138 Previous studies have reported negative correlations between seasonal variations in pH and water
139 temperature, mainly because of changes in the dissociation constant [in dissociation equilibrium](#)
140 $(H_2O \leftrightarrow H^+ + OH^-)$; the pH values were lowest in summer and highest in winter, in both the open
141 ocean (e.g. Bates et al. 2014) and coastal [sea](#) waters (e.g., Frankignoulle and Bouquegneau 1990; Byrne
142 et al. 2013; Hagens et al. 2015; Challener et al. 2016). We therefore assumed that the minimum and
143 maximum pH data coincided with the highest and lowest temperatures, respectively (Fig. 2), and we
144 used these data to calculate pH₂₅ in Section 4.2. [NIES do not discriminate surface \(0.5m – 2m\) and](#)
145 [subsurface \(10 m\) data when they calculate annual maximum and minimum pH, so it is speculated that](#)
146 [annual maximum pH substantially represents winter pH of surface waters, while annual minimum pH](#)
147 [represents summer pH of subsurface waters.](#)

148 The monitoring operations were carried out by licensed operators as outlined in the annual plan of
149 the Regional Development Bureau of each prefecture. These specific licensed operators were retained
150 for the duration of the measurement period, which means that the same laboratories were always in
151 charge of collecting the data. This approach helps to prevent systematic errors that might arise both
152 between measurement facilities and over time, and ensures the datasets are accurate.

153

154 2.2 Quality control procedures and assessing the consistency of the WPCL monitoring data

155 We [selected all the data for fixed sites in coastal sea waters](#) that had continuous time-series from
156 1978 to 2009. There were 2463 regular and non-regular monitoring sites in 1978 and 2127 sites in

157 2009. While there were few sites in some prefectures in Hokkaido and Tohoku, the monitoring sites
158 covered almost all the coastline in Japan (Fig. 1).

159 As explained in more detail later in this section, we applied a three-step quality control procedure.
160 We excluded 1) discontinuous time sequences, 2) time sequences that had extreme outliers in each year,
161 and 3) time sequences that included significant random errors and which were only weakly correlated
162 with time sequences at adjacent sites.

163 When we excluded the sites that had discontinuous time sequences of $\text{pH}_{\text{insitu}}$ from 1978 to 2009,
164 1481 sites remained (Fig. 1). We then excluded time sequences with outliers, defined as sites with data
165 points that were more than three standard deviations from [the average of minimum and maximum](#)
166 $\text{pH}_{\text{insitu}}$ for each year. After this step, 1127 sites remained (not shown). We calculated the trends in the
167 unbroken continuous time sequences of the minimum and maximum $\text{pH}_{\text{insitu}}$ data at each site with
168 linear regression (Fig. 3), and the slopes of the linear regression were taken as the minimum and
169 maximum $\text{pH}_{\text{insitu}}$ trends (e.g. Fig. 3). The linear regression trends might have been influenced by
170 random errors or variations at different temporal scales in the data for each site. To eliminate the
171 influence of these errors and variations as far as possible, we removed the data that had significant
172 random errors, defined as the time sequences for which the standard deviations of $\text{pH}_{\text{insitu}}$ exceeded the
173 average standard deviation of the $\text{pH}_{\text{insitu}}$ time sequences at the 1127 sites. After this step, 302 sites
174 remained (see Fig. 1b for site locations).

175 For the 302 sites, we calculated the correlations of water temperature (Fig. 4a–b) and $\text{pH}_{\text{insitu}}$ (Fig.

176 4c–d) at adjacent monitoring sites in the same prefecture (Fig. 4). At most of the stations, the
177 correlations between the temperatures at the site pairs were relatively strong, which indicates that the
178 temperature followed similar patterns over time at adjacent sites (Fig. 4a–b). The correlations tended
179 to be strong when the sites were close together, but gradually weakened with increasing distance
180 between sites. The patterns in the $\text{pH}_{\text{insitu}}$ and temperature correlations were similar (Fig. 4), which
181 indicates that the $\text{pH}_{\text{insitu}}$ and temperature data at adjacent monitoring sites varied in the same way. In
182 other words, the relative ratios of the measurement errors in $\text{pH}_{\text{insitu}}$ and the natural spatio-temporal
183 variations at these monitoring sites were similar to those for temperature. The absolute values of the
184 $\text{pH}_{\text{insitu}}$ correlation coefficients were slightly lower than those for temperature for each corresponding
185 pair of sites (Figs. 4 and 5), and might reflect the fact that $\text{pH}_{\text{insitu}}$, but not the water temperature, is
186 subjected to strong forcing by coastal biological processes, which causes short-term variations in
187 $\text{pH}_{\text{insitu}}$. The correlations between the minimum $\text{pH}_{\text{insitu}}$ data (Fig. 4c) were weaker than those for the
188 maximum $\text{pH}_{\text{insitu}}$ data (Fig. 4d) because the degree of biological forcing varied by season and was
189 stronger in summer when $\text{pH}_{\text{insitu}}$ was at a minimum and weaker in the winter when $\text{pH}_{\text{insitu}}$ was at a
190 maximum. Despite the influence of biological processes on $\text{pH}_{\text{insitu}}$, the correlation coefficients
191 remained high and were significant ($r=0.367$, $p<0.05$) at most of the monitoring sites, especially at
192 sites that were less than 5 km apart within the same prefecture; at such sites, $\text{pH}_{\text{insitu}}$ followed similar
193 patterns. In the final step of the quality check procedure (step 3), we removed all the time sequences
194 with weak and insignificant correlations for temperature and $\text{pH}_{\text{insitu}}$ (Figs. 4 and 5). After this final

195 step, 289 sites remained.

196 As shown in Table 2, the correlations between temperature and $\text{pH}_{\text{insitu}}$ at sites that were within 15
197 km of each other strengthened after steps 2 and 3, which suggests that the reliability of the dataset
198 improved at each step of the quality control. The mutual correlations among the $\text{pH}_{\text{insitu}}$ and temperature
199 measurements at adjacent sites (Table 2), and the correlations between $\text{pH}_{\text{insitu}}$ trends and TN ones
200 (Table 3) show that the quality control procedures were effective.

201 The monitoring in each prefecture is carried out by different licensed operators, decided by the
202 Regional Development Bureau in each prefecture. *Inter-calibration essays have not been conducted*
203 *between different licensed operators.* Even though all the operators follow the same JIS protocol,
204 manual monitoring can introduce systematic errors into the data. Some adjacent monitoring sites are
205 close to each other but are managed by different operators, such as sites close to the boundaries between
206 Osaka and Hyogo (Fig. 6a), Hyogo and Okayama (Fig. 6b), Kagawa and Okayama (not shown), and
207 Kagawa and Ehime (not shown). The $\text{pH}_{\text{insitu}}$ time sequences for these site pairs were generally similar,
208 even though there were some deviations when compared with the time sequences for adjacent sites
209 within the same prefecture, monitored by the same operator (lines of the same color in Fig. 6). The
210 standard deviations of the $\text{pH}_{\text{insitu}}$ trends between these site pairs close to the boundaries of Osaka and
211 Hyogo, Hyogo and Okayama, Kagawa and Okayama, and Kagawa and Ehime were 0.0014, 0.0012,
212 0.0026, and 0.0017 yr^{-1} , respectively, and were smaller than the acceptable measurement errors of the
213 JIS standard protocols. We can therefore say that the measurements from the different operators in

214 different prefectures were consistent.

215

216 3. Results

217 3.1 Variations in $\text{pH}_{\text{insitu}}$ highlighted by regression analysis

218 The histograms of the calculated $\text{pH}_{\text{insitu}}$ trends (yr^{-1}), for the minimum and maximum $\text{pH}_{\text{insitu}}$ after
219 each quality control step, are shown in Fig. 7. The histogram in Fig. 7a–b shows data of the 1481 sites
220 (discontinuous sites excluded). The data for 1127 sites (i.e., data without outliers from step 2) are
221 shown in Fig. 7c–d, and the data for 289 sites (from step 3) are shown in Fig. 7e–f (Section 2.2). The
222 number of sites decreased at each step of the quality control, but the shapes of the histograms were
223 generally similar for both the minimum and maximum pH trends. The total trends showed overall
224 normal distributions with a negative shift for all the processing level.

225 We detected both positive (basification) and negative (acidification) trends, which contrasts with
226 the findings of other researchers who reported only negative trends (ocean acidification) in the open
227 ocean (Bates et al. 2014; Midorikawa et al. 2010; Olafsson et al. 2009; Wakita et al. 2017). The average
228 (\pm standard deviation) trends for the minimum and maximum $\text{pH}_{\text{insitu}}$ data were -0.0002 ± 0.0061 and
229 $-0.0023 \pm 0.0043 \text{ yr}^{-1}$ for the 1481 sites (Fig. 7a–b), and -0.0005 ± 0.0042 and $-0.0023 \pm 0.0036 \text{ yr}^{-1}$ for
230 the 1127 sites (Fig. 7c–d), respectively. The average trends for the minimum and maximum $\text{pH}_{\text{insitu}}$
231 data for the 289 sites that remained after step 3 were -0.0014 ± 0.0033 and $-0.0024 \pm 0.0042 \text{ yr}^{-1}$,
232 respectively (Fig. 7e–f).

233 The negative trends were relatively weak for the minimum $\text{pH}_{\text{insitu}}$ data and relatively strong for
234 the maximum $\text{pH}_{\text{insitu}}$ data, but there was an overall tendency towards acidification. At the 289 sites,
235 there were 204 negative and 86 positive trends for the minimum $\text{pH}_{\text{insitu}}$ data and 217 and 72 negative
236 and positive trends for the maximum $\text{pH}_{\text{insitu}}$ data. This shows that for the minimum data, there were
237 acidification and basification trends at 70% and 30% of the monitoring sites, respectively, with values
238 of 75% and 25% for the maximum data, respectively.

239

240 3.2 Local patterns in acidification and basification

241 We examined the $\text{pH}_{\text{insitu}}$ trends for the 289 sites for local patterns in acidification and basification
242 (Section 2.2), and found that the trends seemed to be randomly distributed. For example, the values
243 were different at sites that were less than 50 km apart (Fig. 8). There are many monitoring sites in the
244 Seto Inland Sea and in Western Kyushu. The trends for the minimum and maximum $\text{pH}_{\text{insitu}}$ showed
245 both acidification and basification in the Seto Inland Sea (Fig. 8a–b, 8c–d). In the western part of
246 Kyushu, acidification dominated (Fig. 8a–b, 8c–d) and there were few clusters of basification in
247 $\text{pH}_{\text{insitu}}$ for both the minimum and maximum $\text{pH}_{\text{insitu}}$ data (Fig. 8b, d). Figure 8a (b) and Figure 8c (d)
248 are similar, which suggests that, at most of the sites where we detected acidification and basification,
249 the trend directions were consistent for the minimum and maximum $\text{pH}_{\text{insitu}}$ (Fig. 8a–b, 8c–d).

250 By examining the average minimum and maximum $\text{pH}_{\text{insitu}}$ trends in each prefecture (Fig. 9a–b, d–e,
251 g–h, j–k), we found that, while the average values were slightly different, the trends in the averaged

252 values and the patterns in acidification and basification for both the minimum and maximum $\text{pH}_{\text{insitu}}$
253 were the same from north to south and from west to east. We also found acidification trends in most of
254 the prefectures with at least 17 sampling sites, namely Miyagi, Wakayama, Hyogo, Okayama,
255 Yamaguchi, Tokushima, Kagawa, Ehime, and Nagasaki (Figs. 1a and 9c, f, i, l). The average estimates
256 for the maximum $\text{pH}_{\text{insitu}}$ were larger than those for the minimum $\text{pH}_{\text{insitu}}$ in these prefectures.

257 We found more acidification trends for the minimum $\text{pH}_{\text{insitu}}$ in the southwestern prefectures of
258 Yamaguchi, Kagawa, Ehime, Hyogo, and Nagasaki than in the northeastern prefecture of Miyagi (Fig.
259 9a, d, g, i) (see Fig. 1 for locations). The maximum and minimum $\text{pH}_{\text{insitu}}$ trends indicated basification
260 in Wakayama and Okayama prefectures (Fig. 9c). The trends in Osaka, Hyogo, Okayama, Hiroshima,
261 Yamaguchi, Kagawa, and Ehime prefectures (Fig. 1a) were different from each other, even though they
262 were all located in the same part of the Seto Inland Sea (Fig. 9d–e). The trends in Hiroshima and
263 Okayama, within the Seto Inland Sea, were weaker than those in Hyogo, Yamaguchi, Kagawa, and
264 Ehime, which were outside the sea (Fig. 9d–e). The $\text{pH}_{\text{insitu}}$ trend values indicated relatively strong
265 acidification at -0.0025 yr^{-1} in Niigata in the Japan Sea (Fig. 9j–l) but there were fewer than the
266 threshold of 17 monitoring sites in the prefectures.

267

268 4. Discussion

269 4.1 Statistical evaluation of our estimated overall trends

270 The JIS Z8802 (2011) allows a measurement error of ± 0.07 and this treatment further enhanced the

271 uncertainty of the published data to ± 0.1 . The uncertainty of the slope of the linear regression line (σ_β)
272 is estimated by the following equation (e.g., Luenberger 1969):

$$273 \quad \sigma_\beta = \{ \sigma_y^2 / \sum(x_i - [x])^2 \}^{1/2} \quad (1)$$

274 where σ_y^2 is the theoretical variance in a pH value caused by the measurement error (in this case, 0.1^2
275 = 0.01); and x_i and $[x]$ represent the year and the year averaged for all data at a station, respectively.

276 In the WPCL dataset, there are generally 32 data points for each station (for every year from 1978 to
277 2009), spaced at consistent intervals. In this case, $\sum(x_i - [x])^2$ becomes 2728 and σ_β becomes 0.0020
278 yr^{-1} , which is the threshold of significance for the pH trend. This means that our estimated trends
279 included standard deviations that were less than 0.0020 yr^{-1} , and, if there were no trends, a histogram
280 of pH trends should have a normal distribution with an average and standard deviation (σ_β) of 0.0000
281 and 0.0020 yr^{-1} , respectively (Fig. 7). The average trend in the maximum $\text{pH}_{\text{insitu}}$, however, shifted
282 from zero in a negative direction at a rate of more than 0.0020 yr^{-1} for all three scenarios (Fig. 7b, d,
283 f). This result implies that averaged over the whole country, the Japanese coast was acidified in winter
284 to a degree that could be detected from the historical WPCL pH data, even with an uncertainty of ± 0.1 .
285 The observed standard deviation for the maximum $\text{pH}_{\text{insitu}}$ was also larger than the expected value of
286 0.0020 yr^{-1} because of local variations in the pH trends. The average shift in the minimum $\text{pH}_{\text{insitu}}$ data
287 was smaller than 0.0020 yr^{-1} , but all three scenarios showed negative shifts in the average minimum
288 $\text{pH}_{\text{insitu}}$ value (Fig. 7a, c, e).

289 We used Welch's t test to assess the direction of the average minimum and maximum $\text{pH}_{\text{insitu}}$ trends.

290 For our null hypothesis, we assumed that the population of the trends with an average of -0.0014 yr^{-1}
291 (-0.0024 yr^{-1}) and a standard deviation of 0.0033 yr^{-1} (0.0042 yr^{-1}) was sampled from a population
292 with an average trend of 0.0000 yr^{-1} and a standard deviation of 0.0020 yr^{-1} . When the sample size
293 was 289, the t -values and the degrees of freedom were 8.7 (6.2) and 412.2 (474.4), respectively. Since
294 the p value was less than 0.001, the null hypothesis was rejected. Welch's t test confirmed that the
295 average trends for both the minimum and maximum $\text{pH}_{\text{insitu}}$ data were negative.

296 We also applied a paired t -test for the two trends calculated from the averaged minimum and
297 maximum $\text{pH}_{\text{insitu}}$ data, to verify whether two trends are significantly different. The population mean
298 and the sample size were 0.0 and 289, respectively. Since the t -value was calculated to be 4.64 (the
299 degrees of freedom = 288), the null hypothesis was rejected. The paired t -test suggested that the two
300 trends calculated from the averaged minimum and maximum $\text{pH}_{\text{insitu}}$ data are significantly different.

301

302 4.2 Possible influences on the $\text{pH}_{\text{insitu}}$ trends in coastal sea waters

303 To facilitate our discussion of the factors that influenced the $\text{pH}_{\text{insitu}}$ trends, we used the conceptual
304 models of acidification and basification in coastal sea waters of Sunda and Cai (2012) and Duarte et
305 al. (2013), as follows:

$$306 \quad \text{pH}_{\text{insitu}} = \text{Function} (\text{D} (\text{T}), \text{DIC} (\text{Air CO}_2, \text{B} (\text{T}, \text{N})), \text{Alk}(\text{S})) \quad (2)$$

307 The $\text{pH}_{\text{insitu}}$ varies with the ambient temperature (T) on seasonal, inter-annual, and decadal time scales
308 mainly because of changes in the water dissociation constant in dissociation equilibrium (D);

309 $H_2O \leftrightarrow H^+ + OH^-$). Changes in dissolved inorganic carbon (DIC), alkalinity (Alk), and salinity (S)
310 also affect the pH_{insitu} trends. The solubility pump, which is controlled mainly by the atmospheric CO_2
311 concentration (Air CO_2 ; $CO_2 + H_2O \leftrightarrow H^+ + HCO_3^-$), affects DIC, and ocean acidification occurs
312 when the Air CO_2 increases. Dissolved organic carbon can also be affected by biological processes (B)
313 that depend on the ambient temperature (T) and the nutrient loading (N). There are contrasting
314 relationships between DIC and N in heterotrophic and autotrophic oceans. In the waters where primary
315 productivity is predominantly to organic decomposition (i.e., autotrophic water), N increase will
316 enhance primary production and hence decrease DIC, causing basification. In the adjoining waters of
317 this autotrophic water mass (for example, subsurface waters), however, N increase will arise increase
318 of POC (Particle Organic Carbon) transport from the autotrophic water mass, and this leads increase
319 of POC-decomposed DIC (i.e., heterotrophic water) and cause acidification (e.g., Sunda and Cai 2012;
320 Duarte et al. 2013). Alkalinity (Alk) generally varies with salinity (S) in coastal oceans and might also
321 affect the pH_{insitu} trend.

322 The DIC process (Air CO_2) of ocean acidification in equation 2 generally occurred at all monitoring
323 sites when the Air CO_2 concentrations were horizontally uniform, resulting in overall negative trends
324 in minimum and maximum pH_{insitu} . D (T) also has an overall trend of warming in Japan coastal area,
325 and hence made some affections to the observed pH_{insitu} trend. Both the DIC (Air CO_2) and D (T) could
326 be associated with the global processes: ocean acidification and global warming, which were triggered
327 by the increase of CO_2 concentration in the global atmosphere. We will discuss about these global

328 effects focusing on the averages of the whole pH trends in Section 4.2.1.

329 Both DIC (B (T, N)) and Alk (S) are difficult to have general trends that covered all monitoring
330 sites, because factors that control these variables (e.g., salinity of coastal water and terrestrial nutrient
331 loading) have no common trends all over the Japan coast in this dataset. The WPCL data should contain
332 stations of both autotrophic and heterotrophic oceans (Smith and Hollibaugh 1992), and this condition
333 further obscure influence of DIC (B (T, N)) to overall $\text{pH}_{\text{insitu}}$ trend, as the same trend of B (T, N) leads
334 opposite trends of DIC (B (T, N)) in autotrophic and heterotrophic ocean (Duarte et al. 2013). Wide-
335 varying nature of DIC (B (T, N)), and Alk (S) depending on the region might have caused the regional
336 differences of $\text{pH}_{\text{insitu}}$ trends among stations, contributing relatively large standard deviations of both
337 the minimum and maximum $\text{pH}_{\text{insitu}}$ trends (Fig. 7). We will discuss about these local effects associated
338 with the regional differences in Section 4.2.2.

339

340 4.2.1 Global effects on $\text{pH}_{\text{insitu}}$ trends

341 Our analysis was based on the $\text{pH}_{\text{insitu}}$ data, so the difference between the trends might reflect long-
342 term changes in water temperature that affected the dissociation constant (process D (T) in equation 2)
343 or changes in the coastal carbon cycle (including absorption of anthropogenic carbon by the solubility
344 pump, represented by DIC in equation 2) (process DIC (Air CO_2) in equation 2). A part of D (T) and
345 DIC (Air CO_2) effects driven by ocean acidification and global warming could affect the all monitoring
346 sites, and result in the trend distributions with negative shifts.

347 To evaluate the direct thermal effects related to process D (T) in equation 2, we estimated the pH
348 values normalized to 25 deg. C (pH₂₅), assuming that the minimum (maximum) pH_{insitu} and highest
349 (lowest) temperature and other parameters were measured at the same time. By assuming the other
350 parameters that affected the pH calculation in the CO2sys (Lewis and Wallace 1998, csys.m), such as
351 salinity, DIC, and alkalinity, did not change (these parameters are not measured as part of the WPCL
352 program), we used the method of Lui and Chen (2017) to calculate the pH₂₅, as follows:

$$353 \quad \text{pH}_{25} = -\text{pH}_{\text{insitu}} + a_1(T - 25 \text{ deg. C}), \quad (3)$$

354 where a_1 is set to -0.015 and T is the observed temperature.

355 The distributions of the trends in pH₂₅ after applying equation 3 are shown in Fig. 10. The minimum
356 and maximum pH₂₅ data were normally distributed, meaning that the distributions of the pH_{insitu} trends
357 were maintained after applying equation 3 (Fig. 7e, f). The averages (\pm standard deviations) of the
358 minimum and maximum pH₂₅ trends were -0.0010 ± 0.0032 and $-0.0014 \pm 0.0041 \text{ yr}^{-1}$, respectively.
359 The averaged trends are consistent with those reported by Midorikawa et al. (2010), who calculated
360 that pH₂₅ decreased at rates of $-0.0013 \pm 0.0005 \text{ yr}^{-1}$ and $-0.0018 \pm 0.0002 \text{ yr}^{-1}$ in summer and winter
361 from 1983 to 2007 along the 137°E line of longitude in the north Pacific. The asymmetry of the pH₂₅
362 trends between minimum and maximum estimates would be related to the seasonal variations of pCO₂
363 and the associated asymmetric response of air-sea CO₂ flux (Landschutzer et al. 2018; Fassbender et
364 al. 2018).

365 We also used Welch's t test to assess the direction of the averages of minimum and maximum pH₂₅

366 trends, as same as applying it to the $\text{pH}_{\text{insitu}}$ trends. The p value was calculated to be less than 0.001 in
367 this case, so the null hypothesis was again rejected. Welch's t test confirmed that the average trends
368 for both the minimum and maximum pH_{25} data were negative as well, suggesting that the DIC
369 (AirCO_2) effect (i.e. ocean acidification) caused negative shifts of the pH trend distribution after
370 normalizing at 25 deg. C.

371 The pH_{25} and $\text{pH}_{\text{insitu}}$ trends from north to south and from west to east were similar among the
372 prefectures (Fig. 11), except in Miyagi and Tokushima. The trends in the minimum $\text{pH}_{\text{insitu}}$ and summer
373 pH_{25} were quite similar, but the minimum and maximum $\text{pH}_{\text{insitu}}$ trends tended to be more negative (by
374 about -0.0010 yr^{-1}) than the corresponding pH_{25} trends, especially in Wakayama, Hiroshima, Kagawa,
375 and Ehime, which met the threshold number of sampling sites.

376 The average highest temperatures observed at the minimum $\text{pH}_{\text{insitu}}$ were close to 25 deg. C in the
377 regions south of Chiba prefecture (Figs. 1 and 12a–d), so the normalization at 25 deg. C did not much
378 affect the evaluation of the minimum pH_{25} in the southern prefectures. In contrast, the maximum
379 $\text{pH}_{\text{insitu}}$ values were observed at temperatures that were more than 10 deg. lower than 25 deg. C, so the
380 normalization worked well on the winter data. We estimated the temperature trends from the highest
381 and lowest temperatures at the 289 sites that remained after quality control step 3. The trends in the
382 highest and lowest temperatures generally indicated warming, with an average and standard deviation
383 of 0.021 ± 0.040 and $0.047 \pm 0.036 \text{ deg. yr}^{-1}$, respectively (Fig. 13). Estimations from the CO_2sys
384 indicate that these warming trends influenced the pH values and were related to the changes of -0.0004

385 and -0.0010 yr^{-1} in the pH trends in summer and winter, respectively (Fig. 7e–f and 10a–b).

386 We estimated that the $\text{pH}_{\text{insitu}}$ would change from 8.0150 to 8.0147 in summer and from 8.2568 to
387 8.2560 in winter, for temperature changes from 25.00 deg. to 25.02 deg., and from 10.00 deg. to 10.04
388 deg., respectively, for a salinity of 34, DIC of 1900 millimol m^{-3} , and alkalinity of 2200 millimol m^{-3} .
389 The differences between the $\text{pH}_{\text{insitu}}$ and the corresponding pH_{25} trends in summer (-0.0004 yr^{-1}) and
390 winter (-0.0010 yr^{-1}) can be partly explained by the difference between the decrease in the pH trends
391 in summer (-0.0003 yr^{-1}) and winter (-0.0005 yr^{-1}) (Fig. 7e–f) arising from the thermal effects.

392

393 4.2.2 Local effects on $\text{pH}_{\text{insitu}}$ trends

394 We found regional differences in $\text{pH}_{\text{insitu}}$ values itself (e.g. Fig. 6) and $\text{pH}_{\text{insitu}}$ trends (Figs. 8–9).
395 The negative $\text{pH}_{\text{insitu}}$ trends (acidification) were more significant in southwestern Japan than in
396 northeastern Japan, especially for the minimum $\text{pH}_{\text{insitu}}$ data (Fig. 9 and Section 3.2). The JMA (2008,
397 2018) reported that over the past 100 years, the increase in water temperature in western Japan was
398 $\sim 1.30 \text{ deg. C}$ greater than that in northeastern Japan.

399 We used CO2sys (Lewis and Wallace 1998) to predict how $\text{pH}_{\text{insitu}}$ would change under a
400 temperature difference of $0.01 \text{ deg. C yr}^{-1}$ between the northeastern and southwestern areas, and found
401 that pH decreased by $0.0002 (0.0002) \text{ yr}^{-1}$ when the temperature changed from 10.00 deg. C to 10.01
402 deg. C (25.0 deg. to 25.01 deg. C), assuming a salinity of 34, DIC of 1900 millimol/ m^3 , and alkalinity
403 of 2200 millimol/ m^3 . The contrasting trends in the northeast and southwest can be also partly explained

404 by the difference in warming trends (process D (T) in equation 2).

405 The summer $\text{pH}_{\text{insitu}}$ is affected by ocean uptake of CO_2 (process DIC; Bates et al. 2012; Bates 2014)
406 through long-term changes in biological activity (Cai et al. 2011; Sunda and Cai 2012; Duarte et al.
407 2013; Yamamoto-Kawai et al. 2015) as well as the effect of changes in the dissociation constant. The
408 responses of $\text{pH}_{\text{insitu}}$ to changes in marine productivity are, however, complicated.

409 Previous studies have reported that nutrient loadings in Japan have decreased over recent decades
410 (e.g., Yamamoto-Kawai et al. 2015; Kamohara et al. 2018; Nakai et al. 2018), with variable effects on
411 summer $\text{pH}_{\text{insitu}}$ in coastal sea waters. TN was monitored for a shorter period than $\text{pH}_{\text{insitu}}$ (1995 to
412 2009). We assumed that the TN was mainly dissolved inorganic nitrogen, and determined the
413 correlations between TN and the minimum and maximum $\text{pH}_{\text{insitu}}$ data (Fig. 14). There were significant
414 negative correlations between TN and minimum (-0.30) and maximum (-0.29) $\text{pH}_{\text{insitu}}$. These
415 correlations apparently imply that the conditions in most of the monitoring areas of the WPCL
416 programs were heterotrophic. This results also implies that recent decrease of TN loadings had partly
417 offset anthropogenic CO_2 -induced pH decrease in coastal sea waters. However, we should also be
418 careful about the possibility that this may be a result of simultaneous progress of independent two
419 things (i.e., anthropogenic carbon uptake of ocean and decrease of TN loadings in Japan).

420 Nakai et al. (2018) reported that nutrient loadings have decreased in the most parts of the Seto Inland
421 Sea from 1981 to 2010, but several areas remain eutrophic. Because of geographical variations in
422 nutrient loadings and the uneven distribution of autotrophic and heterotrophic water areas, there are

423 significant spatial variations in pH trends in the Seto Inland Sea (Fig. 8). The pH trends in coastal areas
424 of western Kyushu, where the anthropogenic nutrient loadings are relatively low, therefore reflect the
425 decreases in nutrient discharges, resulting in variations between regions (e.g., Nakai et al. 2018;
426 Yamamoto and Hanazato 2015; Tsuchiya et al., 2018). Several cities in this area have introduced
427 advanced sewage treatment to prevent eutrophication in coastal sea waters (Nakai et al. 2018;
428 Yamamoto and Hanazato 2015).

429 **Regional variations** in coastal alkalinity along with salinity might be related to changes in land use
430 and might affect the trends (process Alk(S) in equation 2). Taguchi et al. (2009) measured alkalinity in
431 the surface waters of Ise, Tokyo, and Osaka bays between 2007 and 2009, and reported that total
432 alkalinity was highly correlated with salinity in each bay. For a temperature, salinity, dissolved carbon,
433 and alkalinity of 25.00 deg. C, 35, 1900 millimol m⁻³, and 2300 millimol m⁻³, respectively, pH_{insitu} (=
434 pH₂₅) was estimated at 8.1416 using the CO2sys (Lewis and Wallace 1998). By changing the salinity
435 and alkalinity to 34 and 2200 millimol m⁻³, respectively, pH_{insitu} (= pH₂₅) decreased by 0.0081 to
436 8.0150. This shows that pH could deviate significantly from average trends if the inputs of alkaline
437 compounds are changed; consequently, some of our pH trends could have been affected by changing
438 discharge from different land-use types.

439 Regional differences in pH_{insitu} trends in coastal sea waters might be caused by ocean pollution. The
440 speciation and bioavailability of heavy metals change in acidic waters, causing an increase in the
441 biotoxicity of the metals (Zeng et al. 2015; Lacoue-Labarthe et al. 2009; Pascal et al. 2010; Cambell

442 et al. 2014). The rates at which marine organisms photosynthesize and respire in ocean waters decrease
443 and increase, respectively, in water polluted with heavy metals and oils (process DIC in equation 2)
444 because of biotoxicity and eutrophication, thereby resulting in acidification (Hing et al. 2011; Huang
445 et al. 2011; Gilde and Pinckney 2012).

446

447 5. Conclusions

448 We estimated the long-term trends in $\text{pH}_{\text{insitu}}$ in Japanese coastal sea waters and examined how the
449 trends varied regionally. The long-term $\text{pH}_{\text{insitu}}$ data show highly variable trends, although ocean
450 acidification has generally intensified in Japanese coastal sea waters. We found that the annual $\text{pH}_{\text{insitu}}$
451 minimum (in summer) and $\text{pH}_{\text{insitu}}$ maximum (in winter) decreased at overall rates of -0.0014 and
452 -0.0024 yr^{-1} , respectively, in Japanese coastal sea waters. The averages of the minimum and maximum
453 pH_{25} trends were -0.0010 and -0.0014 yr^{-1} , respectively. The differences between the $\text{pH}_{\text{insitu}}$ and the
454 corresponding pH_{25} trends in summer (-0.0004 yr^{-1}) and winter (-0.0010 yr^{-1}) can be partly explained
455 by the thermal effects. The negative shifts of the pH_{25} trend distributions suggest a signal of ocean
456 acidification in Japanese coastal sea water.

457 There were striking spatial variations in the $\text{pH}_{\text{insitu}}$ trends. Correlations among the $\text{pH}_{\text{insitu}}$ time series
458 at different sites revealed that the high variability in the $\text{pH}_{\text{insitu}}$ trends was not caused by analytical
459 errors in the data but reflected the large spatial variability in the physical and chemical characteristics
460 of coastal environments, such as water temperature, nutrient loadings, and autotrophic/heterotrophic

461 conditions. While there was a general tendency towards coastal acidification, there were positive trends
462 in $\text{pH}_{\text{insitu}}$ at 25%–30% of the monitoring sites, indicating basification, which suggests that the coastal
463 environment might not be completely devastated by acidification. If we can manage the coastal
464 environment effectively (e.g., control nutrient loadings and autotrophic/heterotrophic conditions), we
465 might be able to limit, or even reverse, acidification in coastal areas.

466

467 Acknowledgments

468 We thank the scientists, captain, officers, and personnel of the National Institute for Environmental
469 Studies, Regional Development Bureau of the Ministry of Land, Infrastructure, Transport and Tourism,
470 who contributed to this study. We acknowledge financial support from the Sasakawa Peace Foundation
471 of the Ocean Policy Research Institute. We also appreciate discussions with members of the
472 Environmental Variability Prediction and Application Research Group of the Japanese Agency for
473 Marine-Earth Science and Technology. Suggestions by two reviewers helped us to improve an earlier
474 version of the manuscript.

475

476 References

- 477 Bates, N. R.: Interannual variability of the ocean CO_2 sink in the subtropical gyre of the North Atlantic
478 Ocean over the last 2 decades, *J. Geophys. Res.* 112, C09013, doi:10.1029/2006JC003759, 2007.
- 479 Bates, N. R.: Multi-decadal uptake of carbon dioxide into subtropical mode waters of the North
480 Atlantic Ocean. *Biogeosciences* 9:2, 649–2, 659, <http://dx.doi.org/10.5194/bg-9-2649-2012>, 2012.
- 481 Bates, N. R., Astor, Y. M., Church, M. J., Currie, K., Dore, J. E., Gonzalez-Davila, M., Lorenzoni, L.,

482 Muller-Karger, F., Olafsson, J., and Santana-Casiano, J. M.: A time-series view of changing surface
483 ocean chemistry due to ocean uptake of anthropogenic CO₂ and ocean acidification, *Oceanography*,
484 27 (1):126–141, <http://dx.doi.org/10.5670/oceanog.2014.16>, 2014.

485 Bednarsek, N., Tarling, G. A., Bekker, D. C. E., Fielding, S., Jones, E. M., Venables, H. J., Ward, P.,
486 Kuzirian, A., Leze, B., Feely, R. A., and Murphy, E. J.: Extensive dissolution of live pteropods in
487 the Southern Ocean, *Nature Geoscience Letter*, 5, 881–885, doi: 10.1038/NGEO1635, 2012.

488 Bednarsek, N., Feely, R. A., Reum, J. C. P., Peterson, B., Menkel, J., Alin, S. R., and Hales, B.:
489 *Limacina helicina* shell dissolution as an indicator of declining habitat suitability due to ocean
490 acidification in the California Current Ecosystem, *Proc. R. Soc. B*, 281 20140123, doi:
491 10.1098/rspb.2014.0123, 2014.

492 Borges, A. V. and Gypen, N.: Carbonate chemistry in the coastal zone responds more strongly to
493 eutrophication than to ocean acidification, *Limnology and Oceanography* 55: 346–353, 2010.

494 Montagna, R.: Description and quantification of pteropod shell dissolution: a sensitive bioindicator of
495 ocean acidification, *Global Change Biology*, 18, 2378–2388, doi: 10.1111/j.1365–2486.2012.02668,
496 2012.

497 Byrne, M., Lamare, M., Winter, D., Dworjanyn, S. A., and Uthicke, S.: The stunting effect of a high
498 CO₂ ocean on calcification and development in the urchin larvae, a synthesis from the tropics to the
499 poles, *Philosophical Transactions of the Royal Society B*, 368, 20120439. Doi:
500 10.1098/rstb.2012.0439, 2013.

501 Cai ,W., Hu, X., Huang, W., Murell, M. C., Lehrter, J. C., Lohrenz, S. E., Chou, W., Zhai, W.,
502 Hollibaugh, J. T., Wang, Y., Zhao, P., Guo, X., Gundersen, K., Dai, M., and Gong, G.: Acidification
503 of subsurface coastal waters enhanced by eutrophication, *Nature Geoscience*, 4, 766–700, 2011.

504 Campbell, A. L., Mangan, S., Ellis, R. P., and Lewis, C.: Ocean acidification increases copper toxicity
505 to the early life history stages of the polychaete *arenicola marina* in artificial seawater, *Environ. Sci.*
506 *Technol.* 48, 9745–9753, 2014.

507 Challenger, R. C., Robbins, L. L., and McClintock, J. B.: Variability of the carbonate chemistry in a
508 shallow, seagrass-dominated ecosystem: implications for ocean acidification experiments, *Marine*
509 *and Freshwater Research*, 67, 163–172. Doi:10.1071/MF14219, 2016.

510 DOE (United States Department of Energy): Handbook of methods for the analysis of the various
511 parameters of the carbon dioxide system in sea water; ver. 2, edited by A. G. Dickson and C. Goyet,
512 ORNL/CDIAC-74, 1994.

513 Dore, J. E., Lukus, R., Sadler, D. W., Church, M. J. and Karl, D. M.: Physical and biogeochemical
514 modulation of ocean acidification in the central North Pacific, *Proc. Natl. Acad. Sci.* 106, 12 235–12
515 240, 2009.

516 Doney, S.C., Fabry, V. J., Freely, A., and Kleypas, J. A.: Ocean acidification: The other CO₂ program,
517 *Annu. Rev. Mar. Sci.*, 1, 169–192, 2009.

518 Duarte, C. M., Hendriks, I. E., Moore, T. S., Olsen, Y. S., Steckbauer, A., Ramajo, L., Carstensen, J.,
519 Trotter, J. A., and McCullough, M.: Is ocean acidification an open ocean syndrome? Understanding
520 anthropogenic impacts in seawater pH, *Estuaries and Coasts* 36, 221–236.doi:10.1007/s12237-013-
521 9594-3, 2013.

522 Fassbender J. A., Rodgers B. K., Palevsky I. H., and Sabine L. C.: Seasonal asymmetry in the evolution
523 of surface ocean pCO₂ and pH thermodynamic drivers and the influence on sea-air CO₂ flux, *Global*
524 *Biogeochemical Cycles*, 32, 11476–1497, 2018.

525 Frankignoulle, M., and Bouquegneau, J. M.: Daily and yearly variations of total inorganic carbon in a
526 productive coastal area, *Estuarine, Coastal and Shelf Science* 30, 79–89, 1990.

527 Gattuso, J. P., and Hansson, L.: *Ocean acidification*, Oxford Univ. Press, Oxford, 2011.

528 Glide, K., and Pinckney, J. L.: Sublethal effects of crude oil on the community structure of estuarine
529 phytoplankton, *Estuar. Coasts* 35, 853–861, 2012.

530 Gonzalez-Davila, M., Santana-Casiano, J. M., and Gonzalez-Davila, E. F.: Interannual variability of
531 the upper ocean carbon cycle in the northeast Atlantic Ocean, *Geophys. Res. Lett.* 34, L07608,
532 doi:10.1029/2006GL028145, 2007.

533 Hagens, M., Slomp, C. P., Meysman, F. J. R., Seitaj, D., Harlay, J., Borges, A. V., and Middelburg, J.
534 J.: Biogeochemical processes and buffering capacity concurrently affect acidification in a seasonally
535 hypoxic coastal marine basin, *Biogeoscience* 12, 1561–1583. Doi:10.5194/bg-12-1561-2015, 2015.

536 Hing, L. S., Ford, T., Finch, P., Crane, M., and Morritt, D.: Laboratory stimulation of oil-spill effects
537 on marine phytoplankton, *Aquat. Toxicol* 103, 32–37, 2011.

538 Huang, Y. J., Jiang, Z. G., Zeng, J. N., Chen, Q. Z., Zhao, Y. Q., Liao, Y. B., Shou, L., and Xu, X. Q.:
539 The chronic effects of oil pollution on marine phytoplankton in a subtropical bay, China. *Environ.*
540 *Monit. Assess.* 176, 517–530, 2011.

541 Intergovernmental Panel on Climate Change (IPCC): *Climate Change 2013: The Physical Science*
542 *Basis. Contribution of Working Group I to the Fifth Assessment Report of the Intergovernmental*
543 *Panel on Climate Change*, ed. Stocker, T. F., Qin, D., Plattner, Gian-Kasper., Tignor, M. M. B., Allen,
544 S. K., Boschung, J., Nauels, A., Zia Y., Bex, V., Midgley, P. M., 1–1535 pp. Cambridge,
545 UK: Cambridge University Press, Cambridge, United Kingdom and New York, NY, USA, 2013.

546 Japanese Industrial Standard Z8802 : <http://kikakurui.com/z8/Z8802-2011-01.html> (in Japanese), 2011.

547 Japanese Meteorological Agency :

548 [http://dl.ndl.go.jp/view/download/digidepo_3011050_po_synthesis.pdf?itemId=info%3Andljp%2F](http://dl.ndl.go.jp/view/download/digidepo_3011050_po_synthesis.pdf?itemId=info%3Andljp%2Fpid%2F3011050&contentNo=1&alternativeNo=&_lang=en)
549 [pid%2F3011050&contentNo=1&alternativeNo=&_lang=en](http://dl.ndl.go.jp/view/download/digidepo_3011050_po_synthesis.pdf?itemId=info%3Andljp%2Fpid%2F3011050&contentNo=1&alternativeNo=&_lang=en), 2008.

550 Japanese Meteorological Agency :

551 https://www.data.jma.go.jp/kaiyou/data/shindan/a_1/japan_warm/japan_warm.html (in Japanese),
552 2018.

553 Kamohara, S., Takasu, Y., Yuguchi, M., Mima, N., and Yoshunari, A.: Nutrient decrease in Mikawa
554 Bay, *Bulletin of Aichi Fisheries Research Institute* 23, 30–32. (in Japanese), 2018.

555 Keeling, C. D., and Whorf, T. P.: Atmospheric CO₂ concentration—Manoa Loa Observatory, Hawaii,
556 1958-1997 (revised August 1998), ORNL NDP-001, Oak Ridge Natl. Lab. Oak Ridge, TN, 1998.

557 Lacou-Labarthe, T., Martin, S., Oberhansli, F., Teyssie, J. L., Jeffree, R., Gattuso, J. P., and
558 Bustamante, P.: Effects of increased pCO₂ and temperature on tracer element (Ag, Cd and Zn)
559 bioaccumulation in the eggs of the common cuttlefish, *Sepia officinalis*. *Biogeosciences* 6,
560 2561–2573, 2009.

561 [Landschutzer P, Gruber N, Bakker C. E. D., Stemmler I, Six D. K.: Strengthening seasonal marine](#)
562 [CO₂ variations due to increasing atmospheric CO₂. *Nature Climate Change*, 8, 146–150, 2018.](#)

563 Lemasson, A. J., Fletcher, S., Hall-Spence, J. M., and Knights, A. M.: Linking the biological impacts
564 of ocean acidification on oysters to changes in ecosystem services: A review, *Journal of Experimental*
565 *Marine Biology and Ecology*, 492, 49–62, 2017.

566 Lewis, E., and Wallace, D. W. R.: Program Developed for CO₂ System Calculations. ORNL/CDIAC-
567 105. Carbon Dioxide Information Analysis Center, Oak Ridge National Laboratory, U.S. Department
568 of Energy, Oak Ridge, Tennessee, 1998.

569 Luenberger, D. G.: Optimization by vector space methods, pp. 1-326, John Wiley & Sons, Inc., New
570 York, N.Y, 1969.

571 Lui, H., and Chen, A. C.: Reconciliation of pH₂₅ and pH_{insitu} acidification rates of the surface oceans:
572 A simple conversion using only in situ temperature, *Limnology and Oceanography: methods*, 15,
573 328–355, doi:1002/lom3.10170, 2017.

574 Midorikawa, T., Ishii, M., Sailto, S., Sasano, D., Kosugi, N., Motoi, T., Kamiya, H., Nakadate, A.,
575 Nemoto, K., and Inoue, H.: Decreasing pH trend estimated from 25-yr time series of carbonate
576 parameters in the western North Pacific, *Tellus*, 62B, 649–659, doi:
577 10.1111/j.1600–0889.2010.00474.x, 2010.

578 Ministry of the Environment: <http://www.env.go.jp/hourei/05/000140.html> (in Japanese), 2018.

579 Nakai, S., Soga, Y., Sekito, S., Umehara, S., Okuda, T., Ohno, M., Nishijima, W., and Asaoka, S.:
580 Historical changes in primary production in the Seto Inland Sea, Japan, after implementing
581 regulations to control the pollutant loads, *Water Policy* wp2018093. Doi:10.2166/wp.2018.093, 2018.

582 National Institute for Environmental Studies :

583 https://www.nies.go.jp/igreen/explain/water/content_w.html (in Japanese), 2018.

584 Olafsson, J., Olafsdottir, S. R., Benoit-Cattin, A., Danielsen, M., Arnarson, T. S., and Takahashi, T.:
585 Rate of Iceland Sea acidification from time series measurements, *Biogeosciences* 6:2, 661–2, 668,
586 <http://dx.doi.org/10.5194/bg-6-2661-2009>, 2009.

587 Pascal, P. Y., Fleeger, J. W., Galvez, F., and Carman, K. R.: The toxicological interaction between ocean
588 acidity and metals in coastal meiobenthic copepods, *Mar. Pollut. Bull*, 60, 2201–2208, 2010.

589 Sarmiento, J. L., and Gruber, N.: *Ocean Biogeochemical dynamics*, pp. 1-503, Princeton Univ. Press,
590 Princeton, New Jersey; Oxfordshire, United Kingdom, 2006.

591 [Smith, S.V., and Hollibaugh, J. T.: Coastal metabolism and the oceanic carbon balance. Review of](#)
592 [Geophysics](#), 31, 75-89, 1993.

593 Sunda, W. G., and Cai, W. J.: Eutrophication induced CO₂-acidification of subsurface coastal waters:
594 interactive effects of temperature, salinity, and atmospheric pCO₂, *Environ. Sci. Technol.* 46,
595 10651–10659, 2012.

596 Taguchi, F., Fujiwara, T., Yamada, Y., Fujita, K., and Sugiyama, M.: Alkalinity in coastal seas around
597 Japan, *Bulletin on coastal oceanography*, Vol.47, No.1, 71–75, 2009.

598 Yamamoto-Kawai, M., Kawamura, N., Ono, T., Kosugi, N., Kubo, A., Ishii, M., and Kanda, J.: Calcium
599 carbonate saturation and ocean acidification in Tokyo Bay, Japan, *J. Oceanogr.* 71:427–439, doi
600 10.1007/s10872-015-0302-8, 2015.

601 Tsuchiya, K., Ehara, M., Yasunaga, Y., Nakagawa, Y., Hirahara, M., Kishi, M., Mizubayashi, K.,
602 Kuwahara, V. S., and Toda, T.: Seasonal and Spatial Variation of Nutrients in the Coastal Waters
603 of the Northern Goto Islands, Japan, *Bulletin on coastal oceanography*, 55, 125-138. (in
604 *Japanese*), 2018.

605 Yamamoto, T., and Hanazato, T.: Eutrophication problems of oceans and lakes, -fishes cannot live in
606 clean water, pp. 1–208, ChijinShokan Co. Ltd, ISBN978-4-8052-0885-4, (in Japanese), 2015.

607 Yara, Y., Vogt, M., Fujii, M., Yamano, H., Hauri, C., Steinacher, M., Gruber, N. and Yamano, Y. : Ocean
608 acidification limits temperature-induced poleward expansion of coral habitats around Japan,
609 *Biogeosciences*, 9, 4955–4968, doi : 10.5194/bg-9-4955-2012, 2012.

610 Zeng, X., Chen, X., and Zhuang, J.: The positive relationship between ocean acidification and pollution,
611 *Mar. Poll. Bull.* 91, 14–21, 2015.

612 Wakita, M., Nagano, A., Fujiki, T., and Watanabe, S.: Slow acidification of the winter mixed layer in
613 the subarctic western North Pacific, *J. Geophys. Res. Oceans*, 122, 6923–6935,
614 doi:10.1002/2017JC013002, 2017.
615

616 Figure captions

617

618 Fig. 1 Coastal maps and monitoring sites in Japan. Red points in (a) indicate the fixed sites ($n = 1481$)
619 monitored by the Regional Development Bureau of the Ministry of Land, Infrastructure, Transport,
620 and Tourism, and the Ministry of the Environment (Japan) under the WCPL monitoring program. (b)
621 Monitoring sites that met the strictest criterion ($n = 302$).

622

623 Fig. 2 Distributions of the monthly number of data points (N) for (a) maximum and (b) minimum
624 temperatures collected in each prefecture from the 302 most reliable monitoring sites.

625

626 Fig. 3 Examples of (a) acidification (Kahoku Coast in Ishikawa) and (b) basification (Funakoshi Bay
627 in Iwate) trends at monitoring sites. Blue and red colors indicate the annual minimum and maximum
628 $\text{pH}_{\text{insitu}}$ data and their trends, respectively.

629

630 Fig. 4 Correlations of water temperature and $\text{pH}_{\text{insitu}}$ at adjacent monitoring sites in the same prefecture.
631 Thin lines denote significant correlations ($r = 0.12$, degrees of freedom = 283).

632

633 Fig. 5 Scatter plots of correlation coefficients for water temperature and $\text{pH}_{\text{insitu}}$ at adjacent monitoring
634 sites in the same prefecture. Fig. 5a is for the highest temperature and the minimum $\text{pH}_{\text{insitu}}$ data and

635 Fig. 5b for the lowest temperature and maximum $\text{pH}_{\text{insitu}}$ data, respectively.

636

637 Fig. 6 Examples of time-series for annual minimum and maximum $\text{pH}_{\text{insitu}}$ data at adjacent monitoring
638 sites close to the boundaries between (a) Osaka and Hyogo and (b) Kagawa and Ehime. Lines of the
639 same color indicate data collected at the same site. **Thin and bold lines indicate the annual minimum
640 and maximum $\text{pH}_{\text{insitu}}$ data, respectively, at each monitoring sites.** Site locations are included to the
641 right of each panel, with the text color corresponding to the colors in each panel.

642

643 Fig. 7 Histogram of pH trends, represented by $\Delta\text{pH}_{\text{insitu}}$, showing the slopes of the linear regression
644 lines for the annual minimum (left) and maximum (right) $\text{pH}_{\text{insitu}}$ data at each monitoring site. The
645 histograms in (a, b), (c, d), and (e, f) show three scenarios: (a, b) all 1481 available sites with
646 continuous records before quality control, (c, d) 1127 sites without outliers, and (e, f) 289 sites that
647 meet the strictest criterion.

648

649 Fig. 8 Distributions of long-term trends in $\text{pH}_{\text{insitu}}$ ($\Delta\text{pH}_{\text{insitu}}/\text{yr}$) in Japanese coastal **sea** waters. The
650 colors indicate the ranges of acidification (a, c) and basification (b, d). (a, b) and (c, d) are linked to
651 the data used in Figs. 7e and 7f, respectively.

652

653 Fig. 9 (a–b, d–e, g–h, j–k) Average minimum and maximum $\text{pH}_{\text{insitu}}$ trends ($\Delta\text{pH}_{\text{insitu}}/\text{yr}$) in each

654 prefecture. These figures show each side of the Pacific (a–b), the Seto Inland Sea (d–e), the East
655 China Sea (g–h), and the Japan Sea (j–k). The prefecture names are arranged vertically from eastern
656 (northern) to western (southern) areas. Black shading indicate one standard deviation from the
657 average. (c, f, i, l) Number of monitoring sites in each prefecture and the thin dashed line is the
658 threshold value of 17 (i.e., the average number of monitoring sites in all prefectures). The prefectures
659 that meet the threshold are indicated in purple. The figure is based on the results shown in Figs. 7 (e,
660 f) and 8.

661

662 Fig. 10 Same as Fig. 7, but showing the pH_{25} trends at 289 sites (selected by quality control step 3).

663 The value of pH_{25} was estimated using the method of Lui and Chen (2017).

664

665 Fig. 11 (a–b, d–e, g–h, j–k) Same as Fig. 9, but showing the average estimated minimum and
666 maximum pH_{25} trends ($\Delta\text{pH}_{25}/\text{yr}$) for each prefecture. Red lines and points indicate the average
667 minimum and maximum $\text{pH}_{\text{insitu}}$ trends shown in Fig. 9.

668

669 Fig. 12 Average highest and lowest temperatures observed for the minimum and maximum $\text{pH}_{\text{insitu}}$ data
670 for each prefecture. The blue and red lines and shading indicate the average and one standard
671 deviation from the average, respectively. The prefectures that met the threshold of 17 are shown in
672 purple, as in Figs. 9 (c–l) and 11 (c–l).

673

674 Fig. 13 Same as Fig. 7, but showing the highest and lowest temperature trends at 289 sites (selected
675 by quality control step 3).

676

677 Fig. 14 Correlation between trends in total nitrogen (TN) and trends in (a) minimum and (b) maximum
678 $\text{pH}_{\text{insitu}}$. The correlation coefficients are -0.30 and -0.29 for the minimum and maximum $\text{pH}_{\text{insitu}}$,
679 respectively (significance level of 0.05, $r = 0.128$; degrees of freedom = 236).

680

681 Table 1 Number of samples (N) collected at each of the 1481 monitoring sites each year.

682

683 Table 2 Average mutual correlation coefficients among water temperature and $\text{pH}_{\text{insitu}}$ measurements at
684 adjacent monitoring sites in the same prefecture. The averages were calculated from the data for the
685 highest and lowest temperature, and minimum and maximum $\text{pH}_{\text{insitu}}$ within 15 km for the three
686 criteria. We refined the sites using three quality control steps, yielding 1481 (step 1), 1127 (step 2),
687 and 302 (step 3) sites. [Two right columns represent a significant level of 5% and a degree of freedom](#)
688 [for the correlation coefficients of each quality check procedure.](#)

689

690 Table 3 Average correlation coefficients between minimum and maximum $\text{pH}_{\text{insitu}}$ trends and total
691 inorganic nitrogen (TN) ones, respectively. We evaluated this for the data after each quality check

692 procedure. Degrees of freedom in step 1 and 2 are same values, because TN data are not necessarily
693 measured at the whole of pH_{insitu} monitoring sites. The sampling number of monitoring sites at step 1
694 and 2 were therefore the same number. Significant levels of 5% and degrees of freedom are also
695 represented.

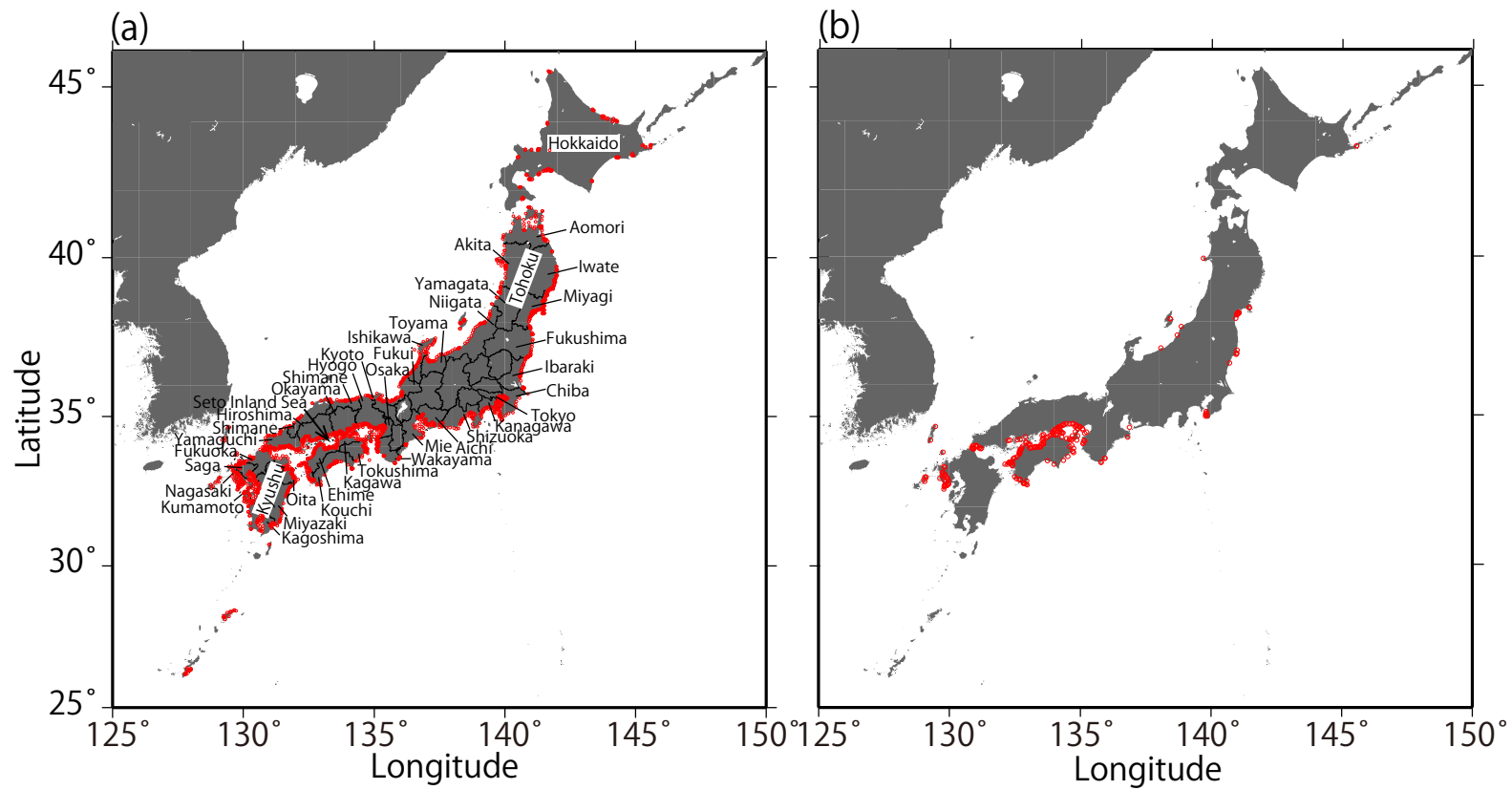


Fig. 1 Coastal maps and monitoring sites in Japan. Red points in (a) indicate the fixed sites ($n = 1481$) monitored by the Regional Development Bureau of the Ministry of Land, Infrastructure, Transport, and Tourism, and the Ministry of the Environment (Japan) under the WCPL monitoring program. (b) Monitoring sites that met the strictest criterion ($n = 302$).

(a) For maximum temperature

(b) For minimum temperature

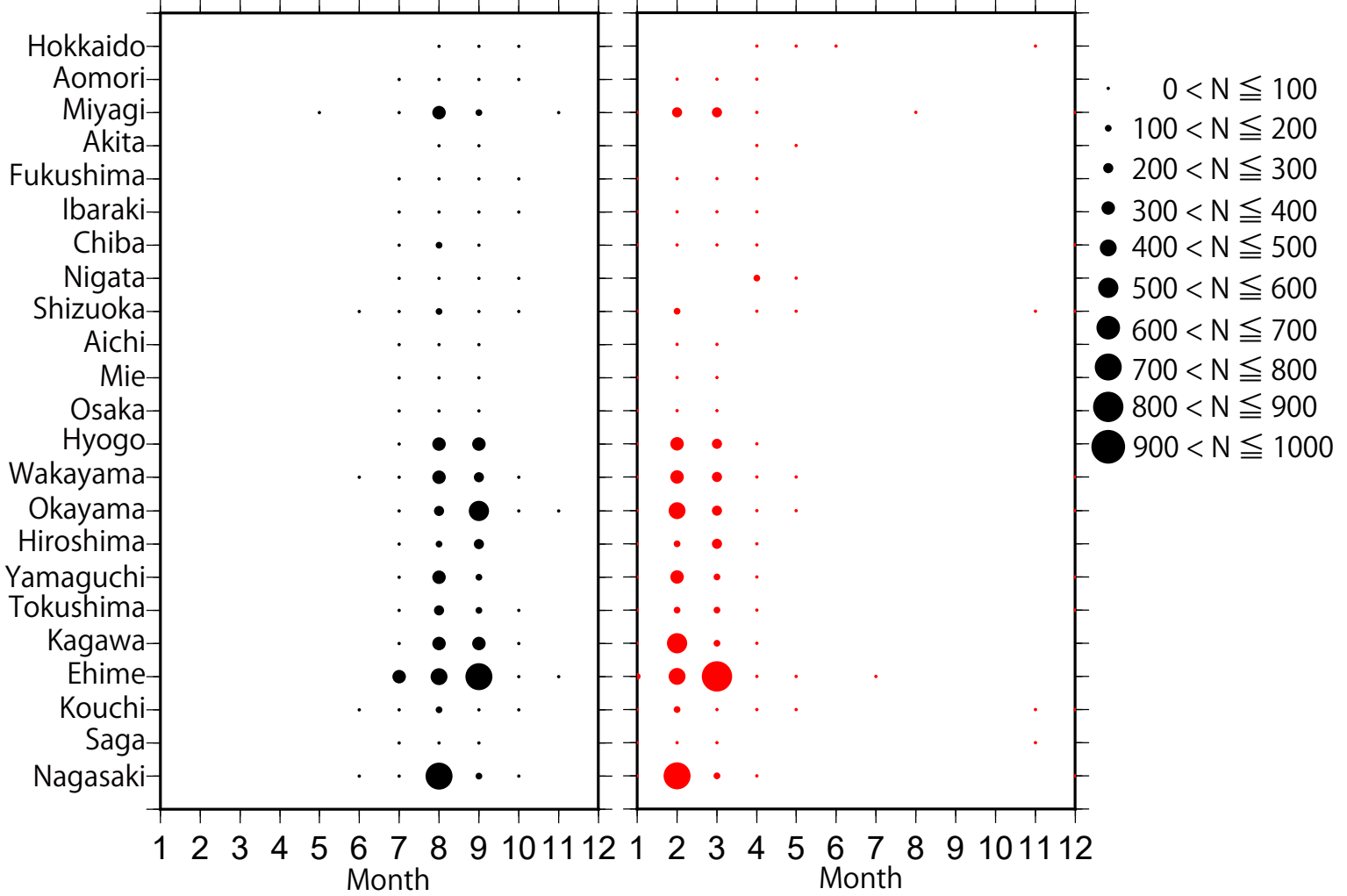


Fig. 2 Distributions of the monthly number of data points (N) for (a) maximum and (b) minimum temperatures collected in each prefecture from the 302 most reliable monitoring sites.

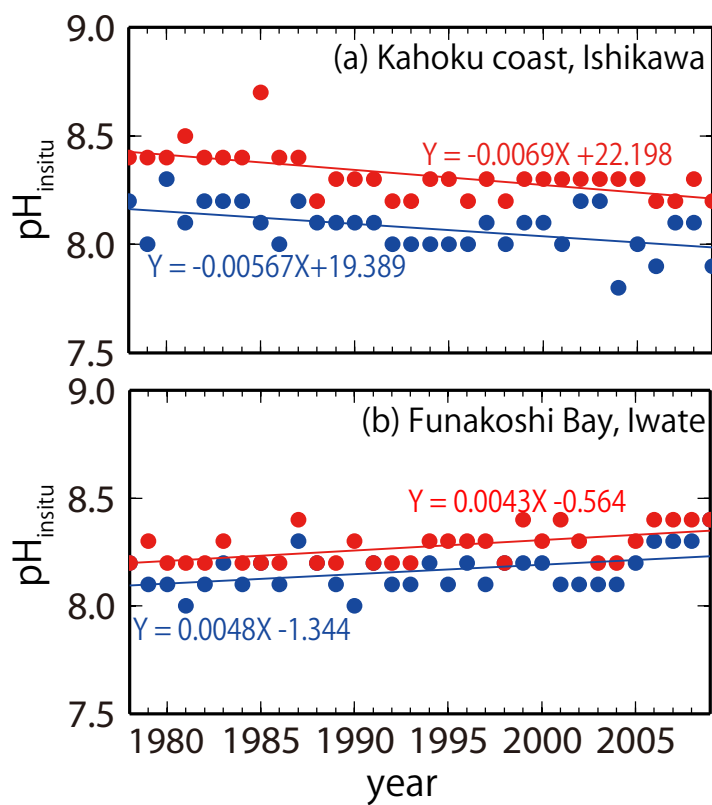


Fig. 3 Examples of (a) acidification (Kahoku Coast in Ishikawa) and (b) basification (Funakoshi Bay in Iwate) trends at monitoring sites. Blue and red colors indicate the annual minimum and maximum pH_{insitu} data and their trends, respectively.

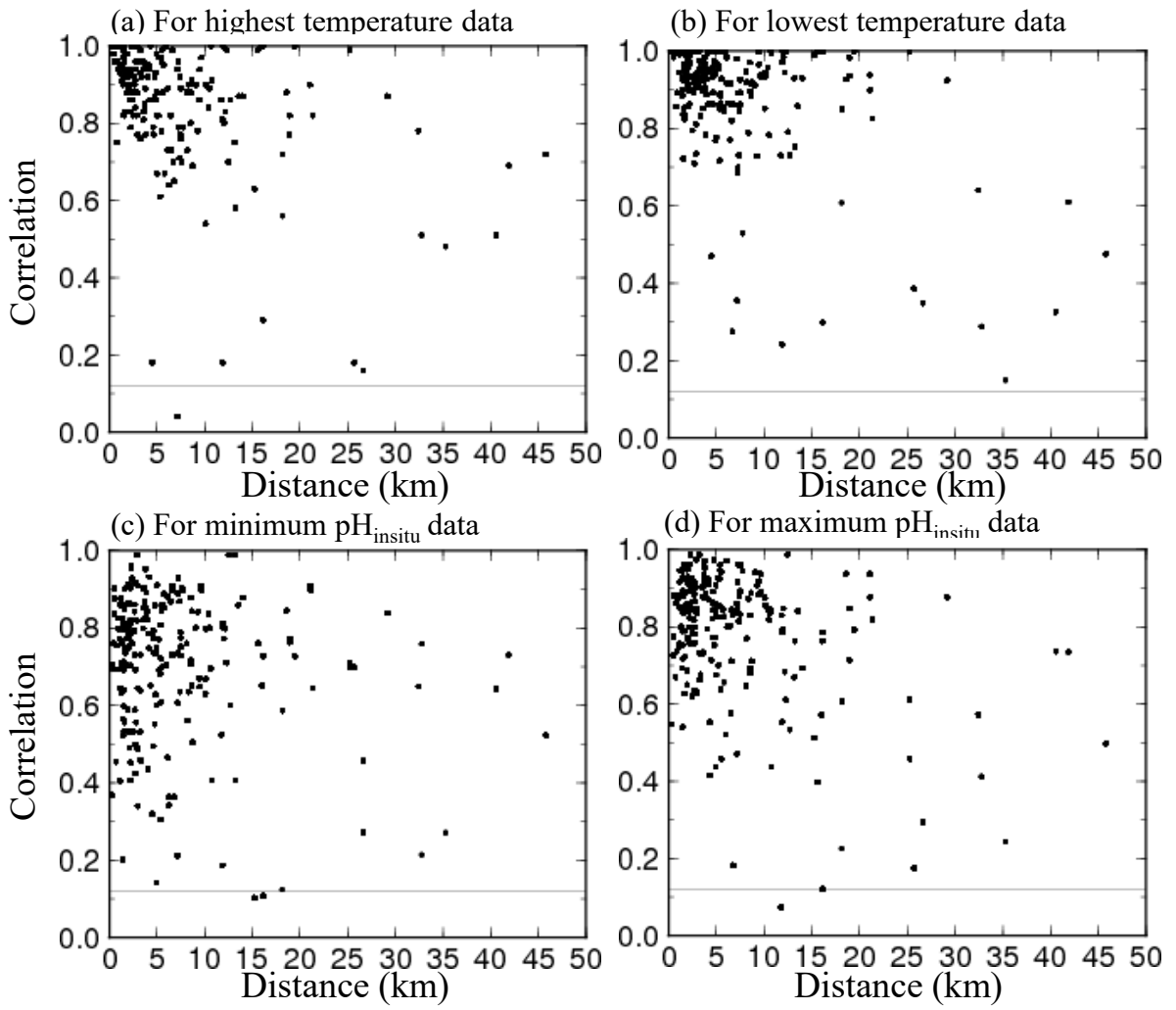


Fig. 4 Correlations of water temperature and $\text{pH}_{\text{insitu}}$ at adjacent monitoring sites in the same prefecture. Thin lines denote significant correlations ($r = 0.12$, degrees of freedom = 283).

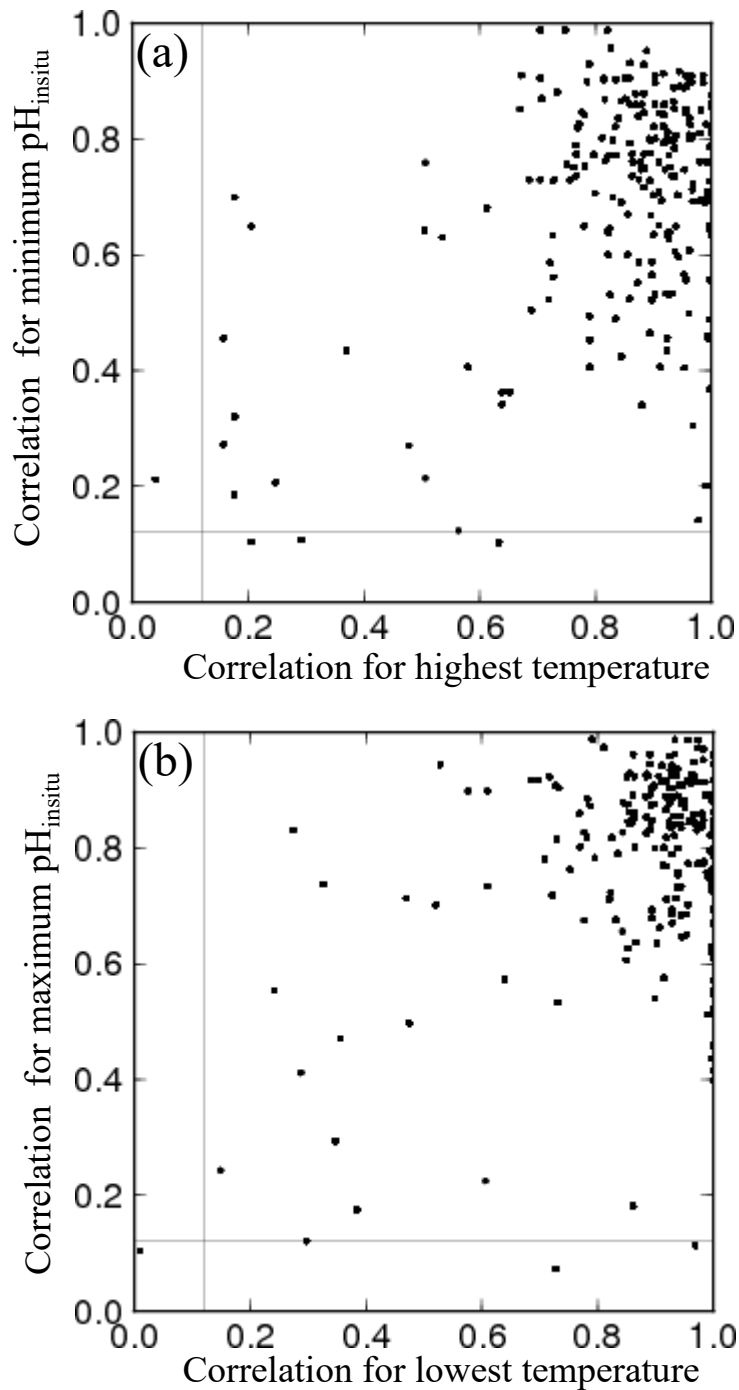


Fig. 5 Scatter plots of correlation coefficients for water temperature and $\text{pH}_{\text{in situ}}$ at adjacent monitoring sites in the same prefecture. Fig. 5a is for the highest temperature and the minimum $\text{pH}_{\text{in situ}}$ data and Fig. 5b for the lowest temperature and the maximum $\text{pH}_{\text{in situ}}$ data, respectively.

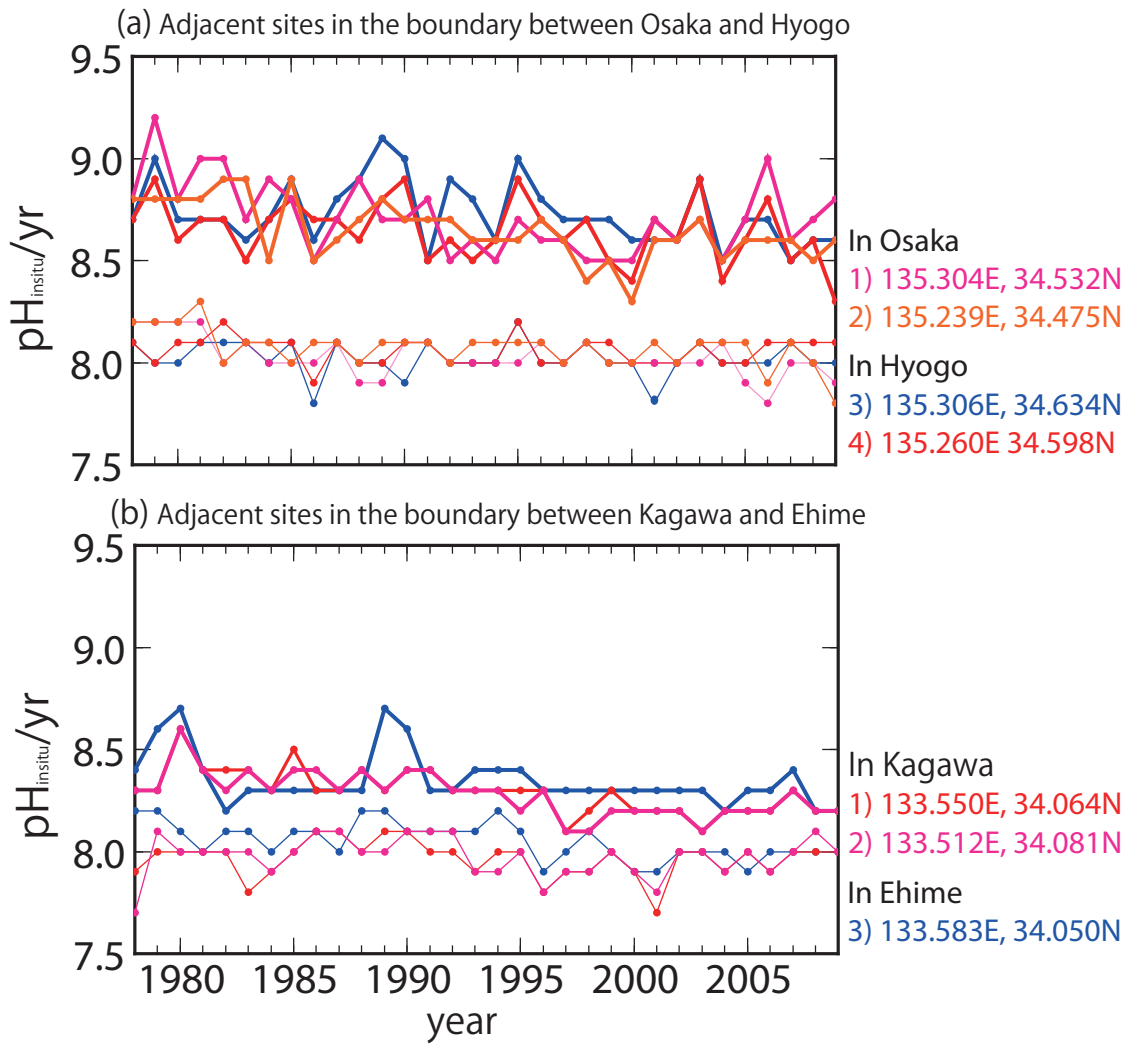


Fig. 6 Examples of time-series for annual minimum and maximum $\text{pH}_{\text{in situ}}$ data at adjacent monitoring sites close to the boundaries between (a) Osaka and Hyogo and (b) Kagawa and Ehime. Lines of the same color indicate data collected at the same site. Thin and bold lines indicate the annual minimum and maximum $\text{pH}_{\text{in situ}}$ data, respectively, at each monitoring stations. Site locations are included to the right of each panel, with the text color corresponding to the colors in each panel.

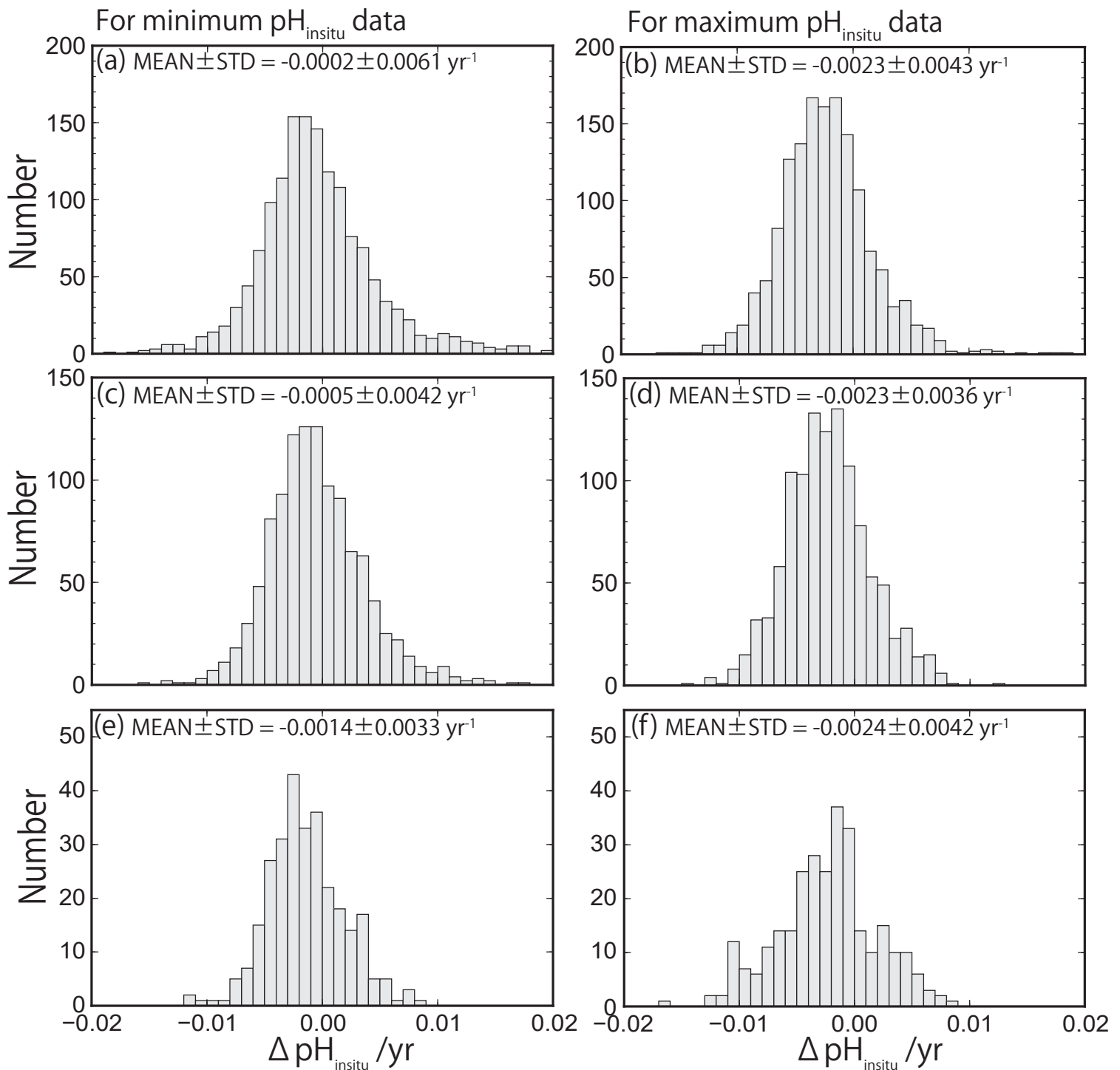


Fig. 7 Histogram of pH trends, represented by $\Delta \text{pH}_{\text{insitu}}$, showing the slopes of the linear regression lines for the annual minimum (left) and maximum (right) $\text{pH}_{\text{insitu}}$ data at each monitoring site. The histograms in (a, b), (c, d), and (e, f) show three scenarios: (a, b) all 1481 available sites with continuous records before quality control, (c, d) 1127 sites without outliers, and (e, f) 289 sites that meet the strictest criterion.

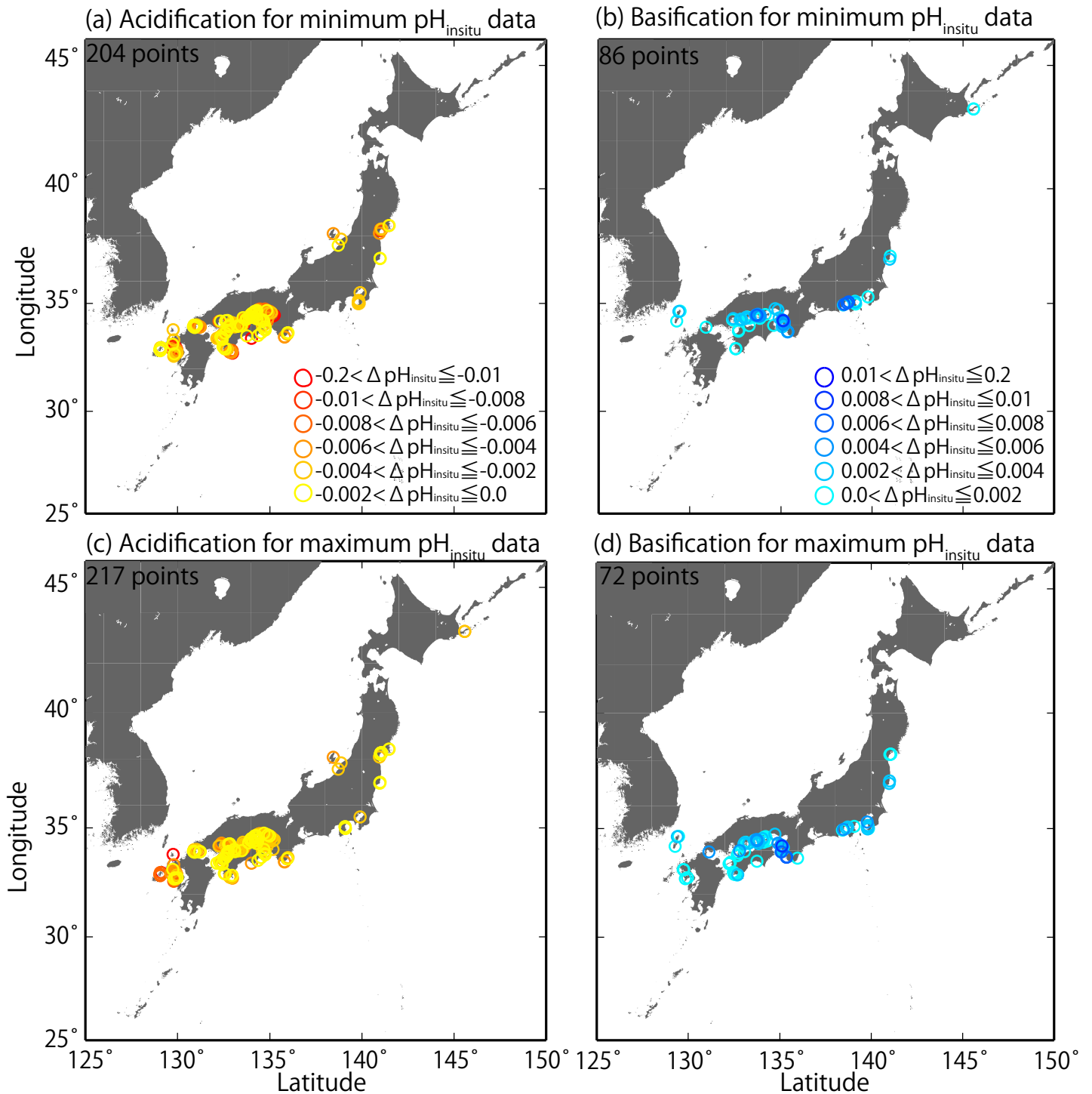


Fig. 8 Distributions of long-term trends in $\text{pH}_{\text{insitu}}$ ($\Delta \text{pH}_{\text{insitu}}/\text{yr}$) in Japanese coastal sea waters. The colors indicate the ranges of acidification (a, c) and basification (b, d). (a, b) and (c, d) are linked to the data used in Figs. 7e and 7f, respectively.

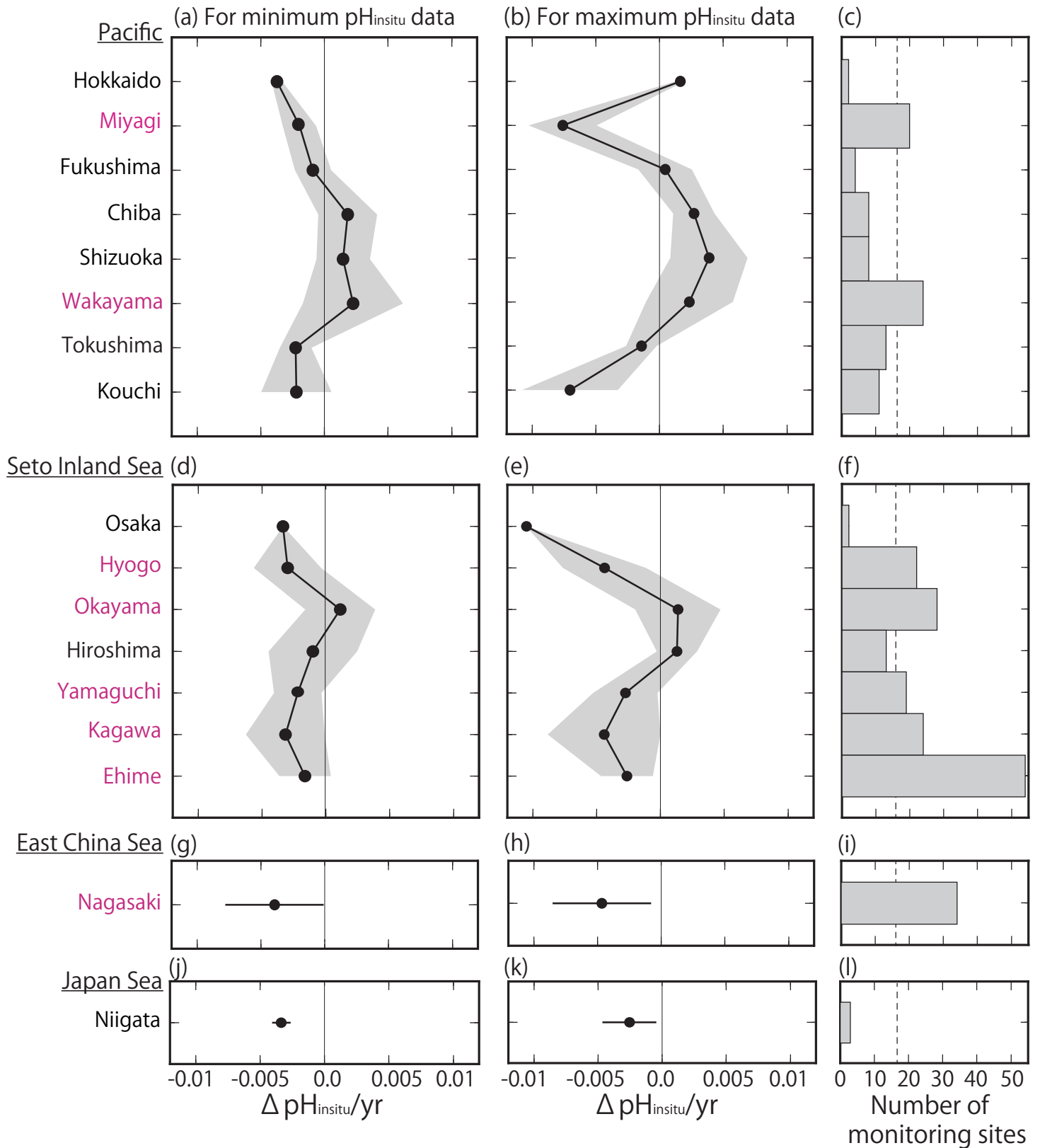


Fig. 9 (a–b, d–e, g–h, j–k) Average minimum and maximum $\text{pH}_{\text{insitu}}$ trends ($\Delta \text{pH}_{\text{insitu}}/\text{yr}$) in each prefecture. These figures show each side of the Pacific (a–b), the Seto Inland Sea (d–e), the East China Sea (g–h), and the Japan Sea (j–k). The prefecture names are arranged vertically from eastern (northern) to western (southern) areas. Black shading indicate one standard deviation from the average. (c, f, i, l) Number of monitoring sites in each prefecture and the thin dashed line is the threshold value of 17 (i.e., the average number of monitoring sites in all prefectures). The prefectures that meet the threshold are indicated in purple. The figure is based on the results shown in Figs. 7 (e, f) and 8.

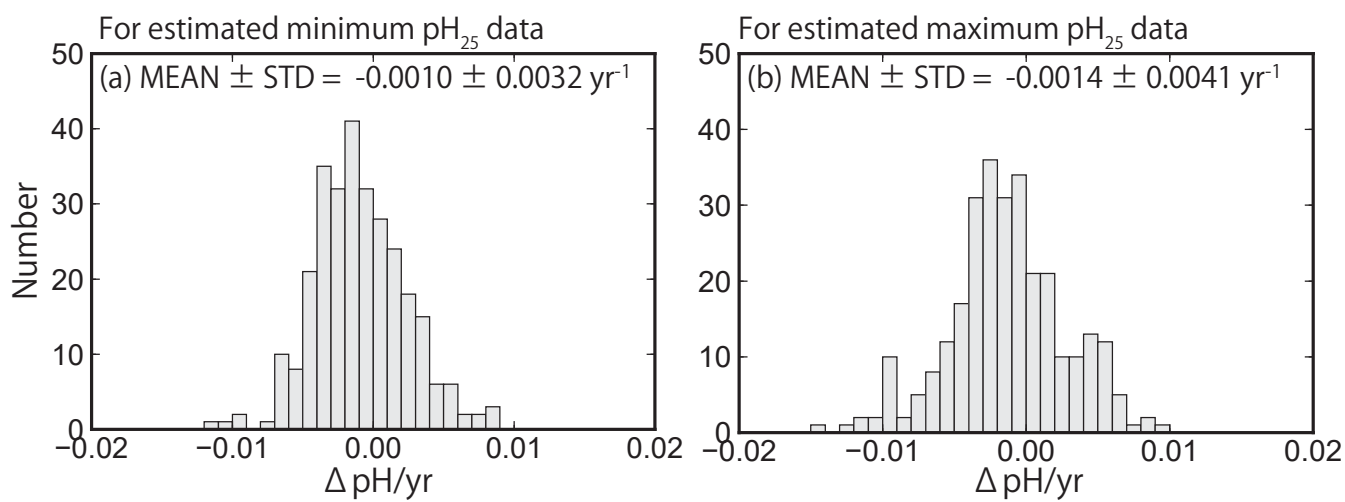


Fig. 10 Same as Fig. 7, but showing the pH_{25} trends at 289 sites (selected by quality control step 3). The value of pH_{25} was estimated using the method of Lui and Chen (2017).

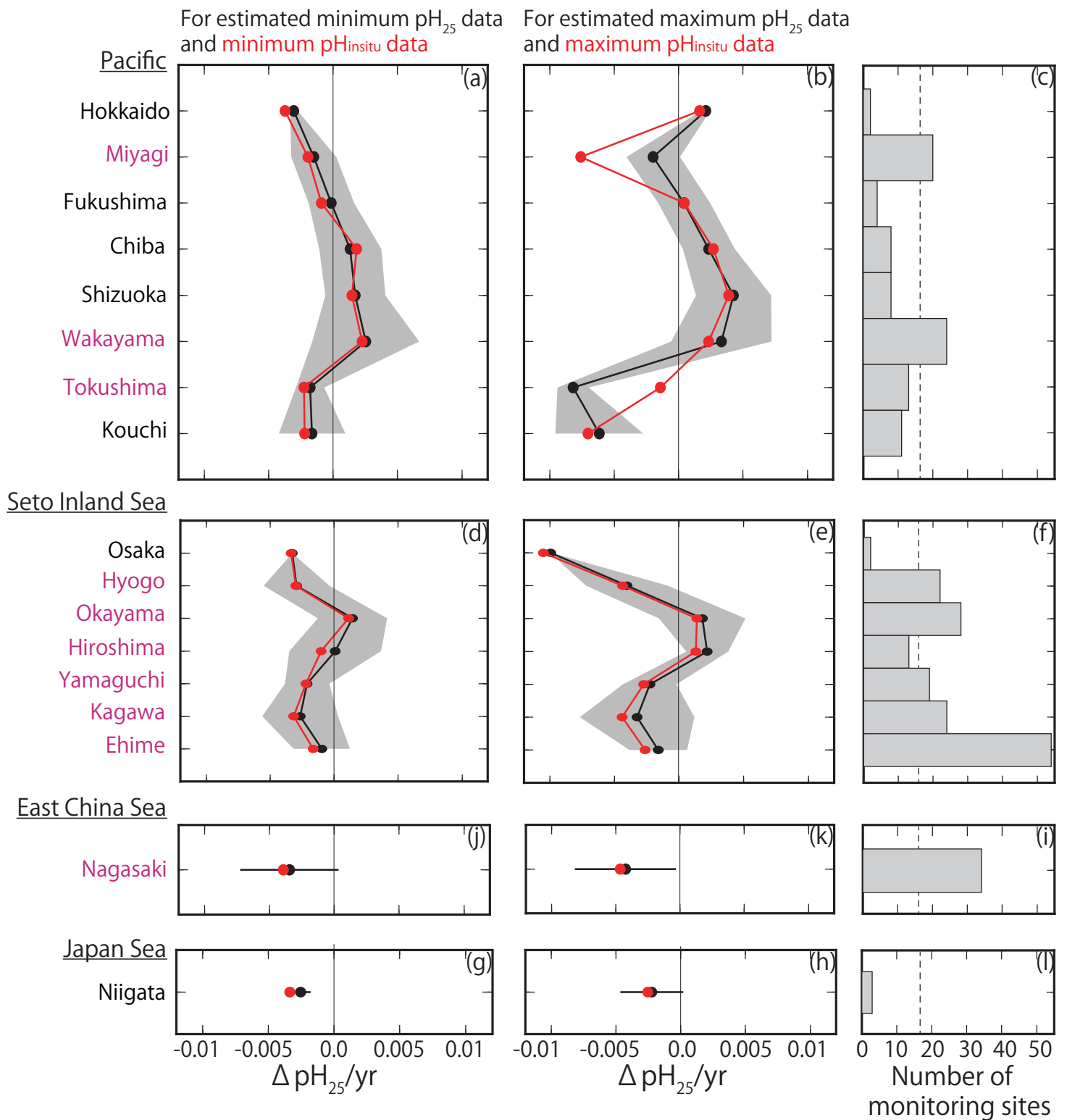


Fig. 11 (a–b, d–e, g–h, j–k) Same as Fig. 9, but showing the average estimated minimum and maximum pH_{25} trends ($\Delta pH_{25}/yr$) for each prefecture. Red lines and points indicate the average minimum and maximum pH_{insitu} trends shown in Fig. 9.

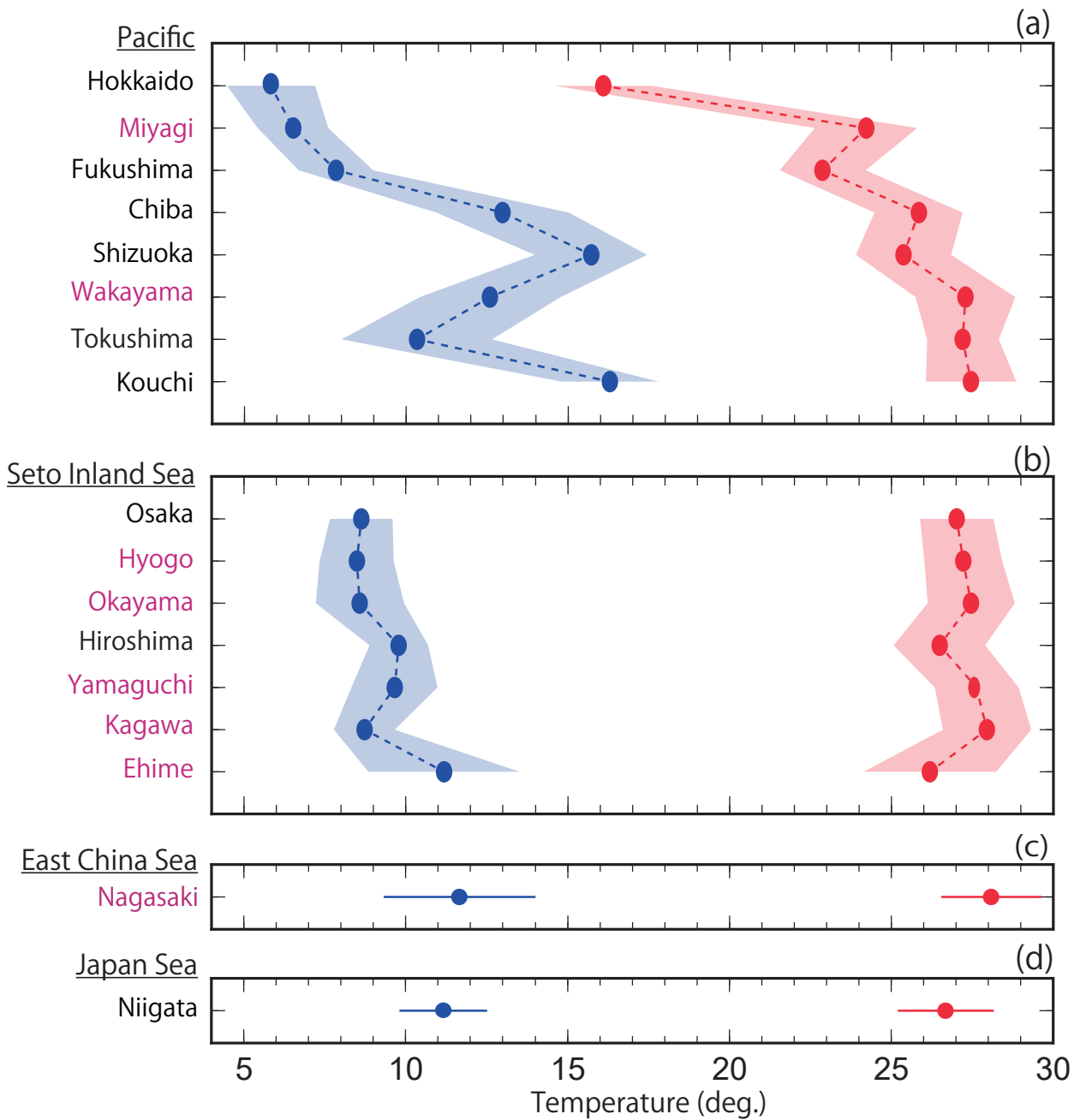


Fig. 12 Average highest and lowest temperatures observed for the minimum and maximum $\text{pH}_{\text{insitu}}$ data for each prefecture. The blue and red lines and shading indicate the average and one standard deviation from the average, respectively. The prefectures that met the threshold of 17 are shown in purple, as in Figs. 9 (c-l) and 11 (c-l).

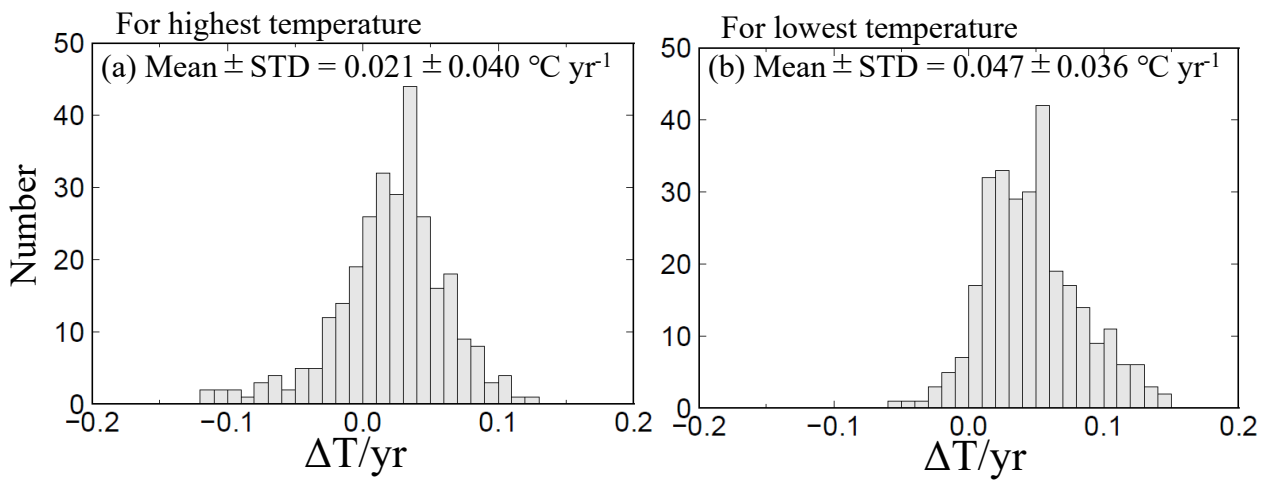


Fig. 13 Same as Fig. 7, but showing the highest and lowest temperature trends at 289 sites (selected by quality control step 3).

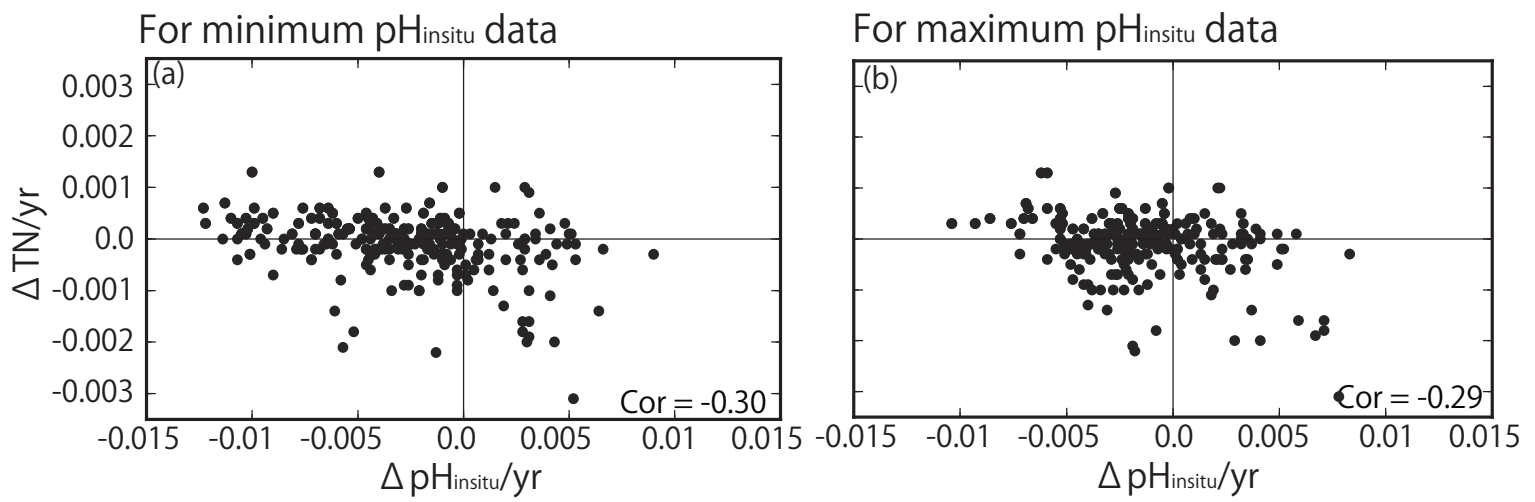


Fig. 14 Correlation between trends in total nitrogen (TN) and trends in (a) minimum and (b) maximum pH_{Insitu}. The correlation coefficients are -0.30 and -0.29 for the minimum and maximum pH_{Insitu}, respectively (significance level of 0.05, $r = 0.128$; degrees of freedom = 236).

Table 1 Number of samples (N) collected at each of the 1481 monitoring sites each year.

Year	$0 \leq N < 4$	$4 \leq N < 8$	$8 \leq N < 12$	$12 \leq N < 16$	$16 \leq N < 20$	$20 \leq N < 24$	$24 \leq N < 28$	$28 \leq N < 32$	$32 \leq N < 40$
1978	43	391	83	303	87	15	176	9	4
1979	31	372	73	328	101	19	150	11	7
1980	32	363	88	324	101	15	192	12	5
1981	24	347	72	361	99	13	199	11	3
1982	25	350	74	364	93	9	206	11	4
1983	32	355	75	356	91	11	222	12	0
1984	28	362	74	355	96	10	211	11	3
1985	24	354	86	377	96	9	192	11	8
1986	25	361	81	334	98	8	235	11	9
1987	26	357	78	341	98	4	239	11	1
1988	25	366	74	356	82	6	236	11	2
1989	26	365	83	344	84	5	238	17	3
1990	24	377	76	347	83	1	238	14	5
1991	24	367	80	355	93	5	226	13	5
1992	24	367	79	352	95	1	230	16	0
1993	17	374	76	357	94	8	225	14	0
1994	17	376	85	347	102	24	208	14	3
1995	29	376	109	311	104	3	227	12	0
1996	19	419	80	307	104	4	226	14	1
1997	20	396	82	315	115	5	225	13	0
1998	16	389	103	325	99	0	225	12	0
1999	17	396	68	381	67	2	224	12	7
2000	17	389	82	376	72	1	231	6	2
2001	17	392	90	382	50	8	220	6	1
2002	17	368	102	392	49	1	229	7	0
2003	17	365	93	402	51	1	233	6	1
2004	17	370	84	400	50	1	240	5	2
2005	16	354	152	356	46	9	228	3	0
2006	16	370	134	345	50	0	244	5	3
2007	17	399	128	353	62	0	202	5	3
2008	17	402	128	350	64	0	211	5	1
2009	17	403	143	340	58	0	217	5	8

Table 2 Average mutual correlation coefficients among water temperature and $\text{pH}_{\text{insitu}}$ measurements at adjacent monitoring sites in the same prefecture. The averages were calculated from the data for the highest and lowest temperature, and minimum and maximum $\text{pH}_{\text{insitu}}$ within 15 km for the three criteria. We refined the sites using three quality control steps, yielding 1481 (step 1), 1127 (step 2), and 302 (step 3) sites. Two right columns represent a significant level of 5% and a degree of freedom for the correlation coefficients of each quality check procedure.

Quality check procedue	highest temperature data	lowest temperature data	minimum $\text{pH}_{\text{insitu}}$ data	maximum $\text{pH}_{\text{insitu}}$ data	Significance level of 5%	Degree of freedom
1	0.79	0.78	0.51	0.64	0.10	386
2	0.80	0.79	0.54	0.69	0.15	170
3	0.85	0.87	0.62	0.72	0.25	59

Table 3 Average correlation coefficients between minimum and maximum $\text{pH}_{\text{in situ}}$ trends and total inorganic nitrogen (TN) ones, respectively. We evaluated this for the data after each quality check procedure. Degrees of freedom in step 1 and 2 are same values, because TN data are not necessarily measured at the whole of $\text{pH}_{\text{in situ}}$ monitoring sites. The sampling number of monitoring sites at step 1 and 2 were therefore the same number. Significant levels of 5% and degrees of freedom are also represented.

Quality check procedue	Correlation between minimum $\Delta \text{pH}_{\text{in situ}}$ and ΔTN	Correlation between maximum $\Delta \text{pH}_{\text{in situ}}$ and ΔTN	Significant level of 5%	Degree of freedom
1	-0.02	-0.29	0.08	622
2	-0.02	-0.29	0.08	622
3	-0.33	-0.35	0.14	215